Aspect Controls on the Spatial Re-Distribution of Snow Water Equivalence through the Lateral Flow of Liquid Water in a Subalpine Catchment

Kori L. Mooney[1,2], Ryan W. Webb[1]

[1]Department of Civil and Architectural Engineering and Construction Management, University of Wyoming, Laramie, WY, 82072, USA
[2]Natural Resources Conservation Service, Salt Lake City, UT, 84138, USA

Correspondence to: Ryan W. Webb (Ryan.Webb@uwyo.edu)

Abstract. Quantifying subalpine snowpack parameters as they vary through time with respect to aspect and position on slope are important for estimating the seasonal storage of snow water resources. Snow depth and density are dynamic parameters that change throughout the progression of the accumulation and melt periods, with direct implications on the distribution of Snow Water Equivalence (SWE) across a landscape. Additionally, changes in density can infer physical processes occurring within the snowpack such as compaction, liquid water ~~pooling~~ponding, and lateral flow. ~~This~~In this study~~ measures~~, we measure snow depth and density throughout the Dry Lake watershed, a 0.25 km^2 watershed in northern Colorado USA using L-Band (1.0 GHz) Ground Penetrating Radar (GPR) and coincident depth probing. ~~GPR snow densities were~~We calibrated these surveys using ~~bulk densities from~~ snow ~~pits~~pit observations and a SNOTEL station. A physical snowpack model, SNOWPACK, with ~~input~~inputs from local Remote Automated Weather Station and a SNOTEL station produced ~~models~~simulations of snow depth, snow density, and liquid water content (LWC). The model simulations indicate mid-winter melt events produced LWC on the south aspect that are less present in the north aspect and flat areas. These midwinter melt events~~ resulted~~, in combination with observations, are interpreted to result in the lateral flow of LWC downslope, and the redistribution of SWE~~ as observed in GPR surveys.~~. Further observations show a steady increase of soil moisture in sensors at the SNOTEL station throughout the winter in the flat terrain and ice layer formation on the south aspect snow pits during mid-winter surveys. Other key observations include ~~pooling~~ponding of liquid water at the base of the north aspect during the later spring season melt phase evidenced by ~~pit observations and~~ GPR transects. We further develop a ~~conceptual~~perceptual model for the aspect controls on the distribution and movement of SWE during the winter and spring seasons. In summary, for the Dry Lake watershed mid-winter melt events are observed on south aspects~~, causing~~ and interpreted to cause a redistribution of SWE downslope while spring melt brings liquid water ~~pooling~~ponding at the base of north aspects. These differences in snowmelt dynamics based primarily on aspect, providing important processes to consider for spatially and temporally extensive SWE measurements moving forward.

1 Introduction

~~Accurately quantifying snow water equivalence (SWE) can provide valuable insight into storage and flux of water resources. SWE can inform spring and summer streamflow generation (Li et al., 2017), soil moisture levels (Mcnamara et al., 2005), and groundwater recharge (Brooks et al., 2021). Additionally, being able to anticipate the timing and quantity of these fluxes can help predict flooding, drought, streamflow volumes, and reservoir storage (Zeinivand and De Smedt, 2010; Modi et al., 2022; Bishay et al., 2023). Regional distributions in SWE also impact ecosystem services through surface albedo, effectively cooling earth surfaces and regulating climate (Sturm et al., 2017). All of these contribute to functioning societies and ecosystems, making the accurate, precise, and timely measurement of SWE an essential annual metric (Mankin et al., 2015). Rapidly shifting global patterns in moisture delivery contribute to measuring SWE in snow-dominated catchments even more important with snowpack parameters changing rapidly in response to shifting weather and climate patterns, even in high elevation snowpacks (Clow, 2010; Nolin et al., 2021). The rapidly changing metrics include snow extent, SWE volume, melt out date, precipitation phase, quantity and magnitude of snowfall events, and surface albedo (Clark et al., 2011; Clow, 2010; Erickson et al., 2005; Painter et al., 2016; Skiles et al., 2018).~~

~~SWE has been measured since the early 1900s through manual snow courses, and later using weather station networks like SNOTEL in the western United States. These sites use snow pillows, snow depth sensors, soil moisture, and precipitation gauges to measure seasonal snow fluxes. With sites scattered across high accumulation areas in the United States, these data provide a statistical estimate of water resources based on the relationship between SWE and streamflow. Forecasts have historically been made based on where the water year fits into the period of record, which gives limited context in accounting for long term trends in hydroclimate and deviation from climate stationarity (Sturm et al., 2017; Bales et al., 2006). Thus, the expansion of snowpack monitoring is necessary to account for spatial and temporal variability found in mountainous environments (Painter et al., 2016; Fassnacht, 2021).~~

Accurately quantifying the spatial and temporal variability of snow water equivalence (SWE) can provide valuable insights for water resources. The variability of SWE can inform spring and summer streamflow generation (Li et al., 2017), soil moisture levels (Mcnamara et al., 2005), and groundwater recharge (Brooks et al., 2021). Additionally, the timing and quantity of runoff from snowmelt can help predict flooding, drought, streamflow volumes, and reservoir storage (Zeinivand and De Smedt, 2010; Modi et al., 2022; Bishay et al., 2023). SWE is commonly measured using weather station networks like the SNOTEL network in the western United States that utilize snow pillows, snow depth sensors, soil moisture, and precipitation gauges. However, these sites offer limited use in streamflow forecasting due to them being point measurements and forecast methods not accounting for deviation from climate stationarity (Sturm et al., 2017; Bales et al., 2006). Shifting global patterns in moisture delivery contribute to the increased importance in measuring SWE for snow-dominated catchments (Clow, 2010; Nolin et al., 2021). Thus, the expansion of snowpack monitoring is necessary to account for spatial and temporal variability found in mountainous environments (Painter et al., 2016; Fassnacht, 2021).

Snowpack properties are sensitive to energy balance dynamics, which is typically expressed in four phases: 1) the accumulation phase, 2) the warming phase in which the average snowpack temperature increases towards 0 °C, 3) the ripening phase in which phase changing occurs, but liquid water is retained in the snowpack, and 4) the output phase where further inputs of energy cause melting to leave the snowpack as snowmelt output (Dingman, 2015). Terrain features like aspect can drastically alter the energy balance, especially in mid-latitude regions where sun incidence angle will preferentially expose south aspects to shortwave radiation during the day (Molotch and Meromy, 2014; Hinckley et al., 2014; Erickson et al., 2005). Canopy is another feature that can alter snowpack energy balance (Musselman et al., 2008; Webb, 2017). Canopies can prolong melt by shielding snow from shortwave radiation (Musselman et al., 2012; Varhola et al., 2010; Lundquist et al., 2013). Canopy will also influence the wind redistribution of snow, increasing the variability of snow accumulation and melt (Mcgrath et al., 2019; Webb et al., 2020b). Similarly, topography can influence wind sheltering and redistribution (Elder et al., 1991; Marks et al., 2002; Winstral et al., 2002). Once the snowpack melts, hillslope processes and soil texture will influence the hydrologic flow paths that form (Webb et al., 2018a; Hinckley et al., 2014; Jencso and Mcglynn, 2011).

The snowmelt input for hydrologic response will rely on the spatio-temporal distribution of SWE, often collected through surveys. Snowpack properties such as bulk snow density are often assumed to be relatively uniform across landscapes based off storm accumulation patterns which can be predicted by air temperature (Valt et al., 2018). Snow density is commonly measured by massing a known volume of a cylinder or a triangular prism, which can be completed as a snow course survey with a federal sampler, or with other tools in a snow pit (Kinar and Pomeroy, 2015). Additionally, dry snow density can be derived from dielectric permittivity (Kovacs et al., 1995; Webb et al., 2021b), which measures the resistance of a medium to the formation of an electric field. Permittivity defines the velocity that a radar wave will travel through a medium such as snow, allowing active radar systems to estimate bulk snow density. Permittivity may also be used to estimate bulk snow liquid water content (LWC), provided an estimate of dry snow density or bulk density is available (Heilig et al., 2015; Koch et al., 2014; Mitterer et al., 2011; Schmid et al., 2015). Thus, ground penetrating radar (GPR) can provide an opportunity to survey spatial patterns with high precision and control over survey locations. Additionally, emerging technologies such as L-Band InSAR depend on knowledge concerning the variability of snowpack properties to constrain uncertainty and improve snow products (Tarricone et al., 2023).

Snowpack properties like snow depth~~, snow cover,~~ and snow surface wetness are increasingly being surveyed using remote sensing techniques like airborne LiDAR, multispectral sensors, and synthetic aperture radar (SAR) ~~(Currier et al., 2019; Painter et al., 2016; Skiles et al., 2018; Tarricone et al., 2023).~~(Currier et al., 2019; Painter et al., 2016; Skiles et al., 2018; Tarricone et al., 2023). These products often work best in-tandem with one another to provide validation, introducing a strong argument for using multiple methods in assessing snowmelt. C-band SAR has been shown as capable of detecting snowmelt and complements snow cover products from Sentinel-2 ~~(Guiot et al., 2023).~~(Guiot et al., 2023). However, the resolution of these products may be limited and unable to capture small scale variability as it is influenced by terrain ~~(Fassnacht et al., 2018).~~(Fassnacht et al., 2018). One example of higher resolution data ~~are those~~is products produced by the Airborne Snow Observatory (ASO) such as spectral albedo, SWE, and depth for basins using LiDAR and multispectral remote sensing platforms ~~(Painter et al., 2016).~~(Painter et al., 2016). These products are appropriate for understanding largescale spatial patterns and resolutions as fine as 3 m; however, these data must rely on modelled snow densities to produce extensive SWE estimates and only represent a brief snapshot in time ~~(Raleigh and Small, 2017). The use of ground-based survey techniques such as ground penetrating radar (GPR) allow surveys at intermediate spatial scales (between point-based stations and airborne platforms) that enable the interpretation of snow properties as they relate to various physiographic controls due to the sensitivity of the radar signal to snowpack properties (Webb, 2017; Mcgrath et al., 2019; Tarricone et al., 2023; Marshall and Koh, 2008; Bonnell et al., 2021; Mcgrath et al., 2022).~~ (Raleigh and Small, 2017). The use of ground-based survey techniques such as GPR allow surveys at intermediate spatial scales (between point-based stations and airborne platforms). When paired with precise measurements of snow depth (d_s), snow dielectric permittivity (ε) can be used to estimate snow density and liquid water content (Sommerfeld and Rocchio, 1993; Kovacs et al., 1995; Webb et al., 2018c; Bonnell et al., 2021; Mcgrath et al., 2022). Because the GPR signal is sensitive to properties such as snow density, GPR surveys enable the interpretation of snowpack properties as they relate to various physiographic controls (Webb, 2017; Mcgrath et al., 2019; Tarricone et al., 2023; Marshall and Koh, 2008; Bonnell et al., 2021; Mcgrath et al., 2022). For these reasons, GPR has been broadly used to observe ε to estimate snow properties (Marshall et al., 2005; Webb, 2017). GPR data can also be collected with minimal disturbance to the snowpack, unlike snow pits, is less time consuming, and d_s observations can be easily be gathered using a depth probe along the same survey track.

~~Snowpack properties are sensitive to energy balance dynamics, which is typically expressed in four phases: 1) the accumulation phase, 2) the warming phase in which the average snowpack temperature increases towards 0 °C, 3) the ripening phase in which phase changing occurs, but liquid water is retained in the snowpack, and 4) the output phase where further inputs of energy cause melting to leave the snowpack as snowmelt output (Dingman, 2015). Terrain features like aspect can drastically alter the energy balance, especially in mid-latitude regions where sun incidence angle will preferentially expose south aspects to shortwave radiation during the day (Molotch and Meromy, 2014; Hinckley et al., 2014; Erickson et al., 2005). Canopy is another terrain feature that can alter snowpack energy balance where subalpine forests reduce accumulation through canopy interception and sublimation (Musselman et al., 2008; Webb, 2017). Conversely, canopies can prolong melt by shielding snow from shortwave radiation (Musselman et al., 2012; Varhola et al., 2010; Lundquist et al., 2013). Canopy will also influence wind redistribution of snow, increasing the variability of snow accumulation and melt (Mcgrath et al., 2019; Webb et al., 2020b). Similarly, topography can influence wind sheltering and redistribution (Elder et al., 1991; Marks et al., 2002; Winstral et al., 2002). Once the snowpack melts, hillslope processes and soil texture will influence the hydrologic flow paths that form (Webb et al., 2018a; Hinckley et al., 2014; Jencso and Mcglynn, 2011).~~

~~Properties such as snow density are often assumed to be uniform across landscapes based off relatively uniform storm accumulation which can be predicted by air temperature (Valt et al., 2018). Snow density is commonly measured by massing a known volume of a cylinder or a triangular prism, which can be completed as a snow course survey with a federal tube sampler, or with other tools in a snow pit. Additionally, dry snow density can be derived from permittivity (Kovacs et al., 1995; Webb et al., 2021b), which measures the resistance of a medium to the formation of an electric field. Permittivity defines~~

~~the velocity that a GPR wave will travel through a medium such as snow. These properties allow active radar systems to measure snow density. Calibrating a snow density model to a specific basin can provide improvement of SWE estimations and has been argued as an important consideration for analyses (Raleigh and Small, 2017; Sexstone and Fassnacht, 2014). GPR provides an opportunity to survey spatial relationships with high precision and control over survey location. Additionally, emerging technologies such as L-Band InSAR depend on knowledge concerning the variability of snowpack properties to constrain uncertainty and improve snow products (Tarricone et al., 2023).~~

~~To assess changes in snow density with aspect and position on a slope, we employ L-Band GPR technology. GPR is a broadly used geophysical imaging technology that uses radar wave reflection patterns to determine media properties like dielectric permittivity (k_s) (Marshall et al., 2005; Webb, 2017). When paired with precise measurements of snow depth (Clark et al.), k_s can be used to calculate snowpack properties such as snow density (Sommerfeld and Rocchio) (Kovacs et al., 1995; Webb et al., 2018c; Bonnell et al., 2021; Megrath et al., 2022). GPR can gather density data with minimal disturbance to the snowpack, unlike snow pits, and is less time consuming, as it is hauled as fast as a surveyor can traverse the snow. Additionally, d_s data can easily be gathered using a depth probe. We use these techniques to answer the following research question: How does snow density and SWE distribution change throughout the snow season based on aspect and relative location on a hillslope?~~

Therefore, to assess seasonal variability in the spatio-temporal distribution of SWE as it relates to energy balance dynamics, we employ L-Band GPR technology to survey snow depth and density with respect to north and south aspect slopes and the relative position on each slope. We use these techniques to answer the following research question: How do variations in snowmelt dynamics impact snow density and SWE distribution throughout the snow season based on aspect and relative location on a hillslope? We aim to answer this question in a manner that will provide insights to snowmelt dynamics for mid-latitude forested mountains that develop a seasonally persistent snowpack.

2 Methods

2.1 Study Site Description

The study site for this research is in the Dry Lake watershed, a small watershed that is ideal for studying snow processes in northern Colorado, USA. The watershed is ~0.25 km^2 with year-round, hourly data collection from a SNOTEL station and a remote automated weather station (RAWS) located within the extents of the watershed~~, respectively (Delong et al.). Elevations range from 2500 to 2660 masl and the primary study area depicted in Figure 1 having~~. Elevations range from 2500 to 2660 meters above sea level (masl) and the primary study area depicted in Figure 1 has a mean elevation of 2545 masl. The SNOTEL station at the site measures a median peak SWE of approximately 510 mm occurring in early April (median date of 10~~-Apr).~~ Apr from 1991 - 2020). Wind direction at Dry Lake is predominantly in the northeast to east direction (Appendix A), parallel to the contours of the north and south aspect hillslopes of the watershed.

The soils in the Dry Lake watershed are ~~primarily loams with very cobbly loam on the south aspect, cobbly sandy loam on the north aspect, and~~ loam on the flatter aspects with observations of highly organic soils in the flat area at the base of the north aspect hillslope~~ (Webb et al., 2018a).~~, cobbly sandy loam on the north aspect, and loam with very cobbly loam on the south aspect (Webb et al., 2018a). A layer of forest litter, or duff layer, also forms on the north aspect hillslope at a depth of approximately 8-15 cm with depths up to 20 cm at the base of the slope. Depth to bedrock ranges from 0.12 m to greater than 1 m with a mean depth to bedrock of 0.40 m. A small stream runs from the northeast to the southwest, with an outlet near the SNOTEL station. The lower area consists of ~~forested conifer~~mixed coniferous trees that is populated with ferns in the summer months and the lower portion of the south aspect is populated by deciduous aspen canopy.

LiDAR data were used to develop terrain and canopy height datasets to quantify the spatial variability of the site ~~(Co, 2016). Using a point cloud filtered for ground surface returns, a 1-meter digital elevation model (DEM) was developed for the site. From the DEM, the~~(Co, 2016). Using a 1-meter digital elevation model (DEM), the flat terrain shares low angle north to west facing surfaces and contains the tallest canopy height resulting in moderate solar radiation (Fig. 1b). The north aspect consists of a mixture of north to west facing surfaces and the south aspect consists of primarily south to southeast facing surfaces. Solar radiation was calculated using the solar radiation tool in ArcGIS Pro for 1 Mar (Fig. 1c).~~ (Fig. 1b).~~ The north aspect has medium to low solar radiation from terrain shading and the highest solar radiation is seen on the south aspect hillslope~~ (Fig.~~ .~~1c).~~ Also from the DEM, the north aspect is slightly steeper than the south aspect~~, particularly at the top of the north aspect survey transect.~~. A ~~second raster was developed from the point cloud which filtered for 1st returns. By differencing the 1-meter DEMs of 1st returns and ground surface returns, ~~canopy height was also calculated (Fig. 1d~~). It is canopied~~) showing denser canopy at the base of the hillslopes, with a shorter sparse canopy at the middle of the north aspect, and open canopy near the top of the north aspect. There is less canopy influence during winter months on the south aspect due to fewer trees and those trees being deciduous species. ~~Relative to the north and south aspects, the flat terrain shares low angle north to west facing surfaces and contains the tallest canopy height resulting in moderate solar radiation is moderate. These spatially variable physiographic parameters are important to consider when dealing with seasonal snowpacks, where the energy balance is sensitive to parameters like terrain and canopy cover shading.~~

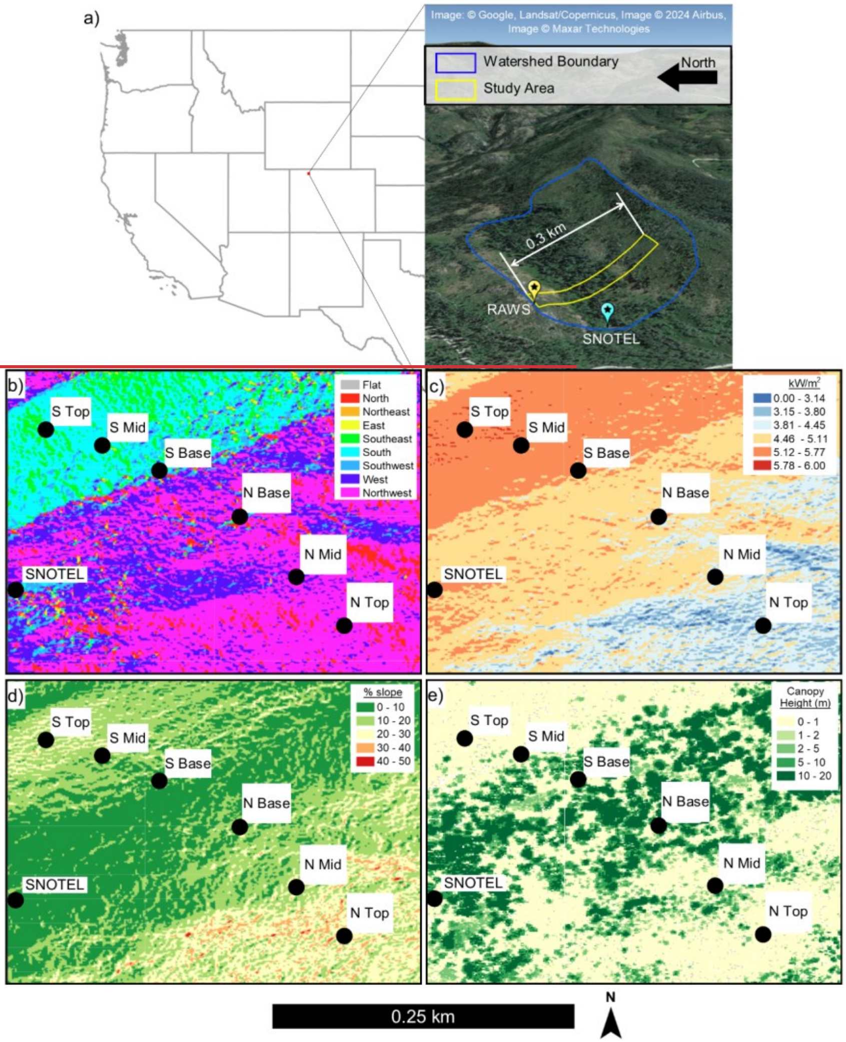

a)
Image: © Google, Landsat/Copernicus, Image © 2024 Airbus, Image © Maxar Technologies
Watershed Boundary
Study Area
North
0.3 km
RAWS
SNOTEL
b)
Flat
North
Northeast
East
Southeast
South
Southwest
West
Northwest
c)
kW/m²
0.00 - 3.14
3.15 - 3.80
3.81 - 4.45
4.46 - 5.11
5.12 - 5.77
5.78 - 6.00
d)
% slope
0 - 10
10 - 20
20 - 30
30 - 40
40 - 50
e)
Canopy Height (m)
0 - 1
1 - 2
2 - 5
5 - 10
10 - 20
S Top
S Mid
S Base
N Base
N Mid
N Top
SNOTEL
0.25 km
N

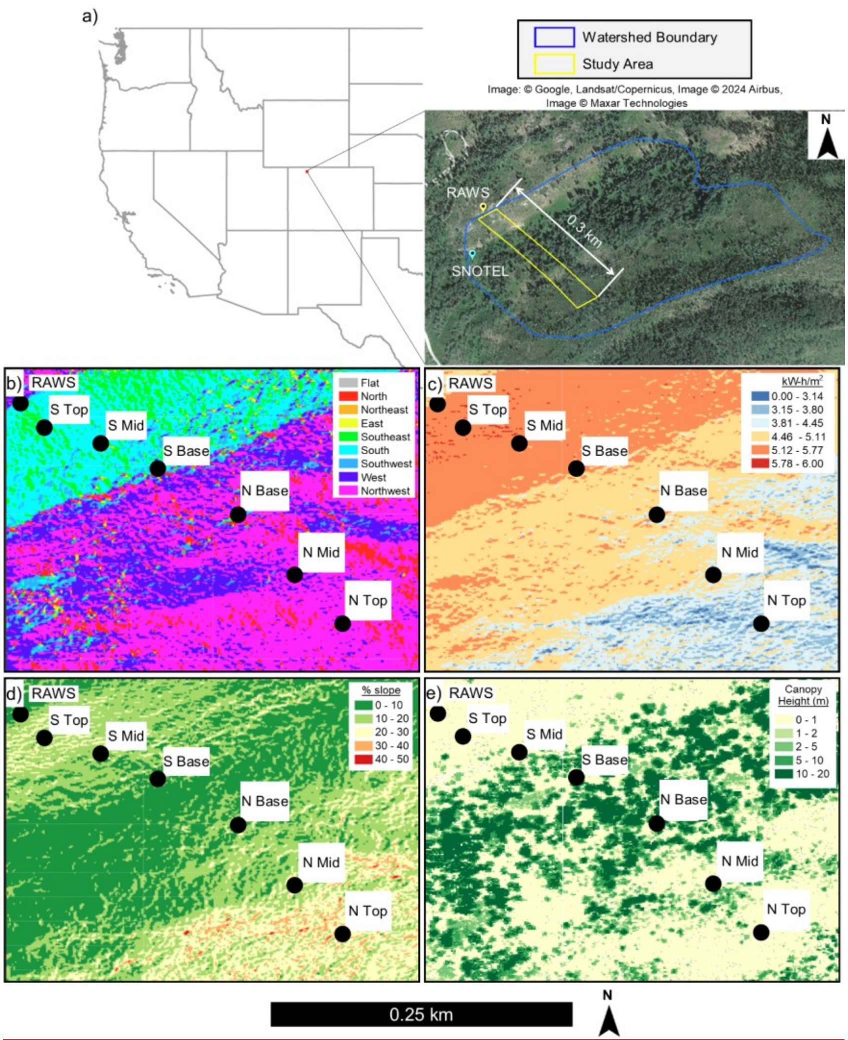

Figure 1: a) The location and imagery of the Dry Lake watershed including general location within the western USA~~, where study area within the watershed where transects were established, and the locations of the RAWS and SNOTEL stations.~~. (Imagery gathered via Google Earth Pro v. 7; Google Earth, 2024; © Google). b) Aspect map, c) solar radiation model for 1 Mar, d) percent slope of terrain, and e) canopy height~~ using LiDAR data~~. Survey transect locations are indicated by black circles.

2.2 Data Collection

In the winter and spring of 2023~~,~~ (12 Jan through 1 May), seven transects were established to collect data at varying positions on the flat, north~~,~~ and south aspects ~~as well as the flat terrain.~~. The spatial distribution of these transects ~~were~~was designed to capture changes in snow properties related to aspect and position on slope including the base, middle, and top of slopes (Fig. ~~2). The~~1). Transects were selected with minimal canopy influence with respect to shading and wind drifts. A flat terrain transect was taken by traversing a circle around the SNOTEL station whereas all other transects were ~20 m in length perpendicular to the fall line (i.e., parallel to slope contours~~, Fig. 2).~~). The base of the north aspect has some shading from coniferous canopy, though shading is predominantly from the terrain at this location, whereas the base of the south aspect has some slight shading from a deciduous canopy. These data were collected approximately once every month from January to May, resulting in ~~5~~five survey dates~~.~~ in 2023 (12 Jan, 6 Feb, 25 Feb, 1 Apr, and 1 May). All transects included GPR data collected with surface-coupled, common offset GPR units pulled over the snow ~~surface~~. The first three surveys used a plastic sled to hold the GPR, ~~and~~whereas the GPR was pulled freely without a sled during the final two surveys. Both ~~systems~~methods of towing were manually towed behind an individual on skis. Two GPR systems were used: a pulseEKKO GPR system for four of the surveys and a Mala Geosciences GPR system~~.~~ during one of the surveys due to the pulseEKKO being at another location at the time of survey. The pulseEKKO system used a shielded antenna at 1000 MHz. The Mala GPR system used a 1600-MHz ~~and 800-MHz antennas~~antenna and was only used during ~~a single late~~the 25 February survey. Following the GPR, depth measurements were collected in the track of the GPR at 2-meter spacing (Webb & Mooney, 2024a). Depending on the length of the transect, the number of depth measurements ranged from 8 to 30 measurements with an average of 13 manually probed d_s measurements to average for each transect area (López-Moreno, 2011).

Snow pits were additionally dug to measure bulk density of the snowpack within the flat terrain, on the north aspect, and at the base of the south aspect (Webb & Mooney, 2024b). GPR transects were conducted next to the ~~pit~~snow pits to calibrate ~~GPR-derived density measurements for~~ each survey date. When time allowed, 1000 cm^3 wedge cutters were used to determine a density profile at 10 cm intervals. During days when time was limited, ~~a profile of~~ ~50 cm long cores with ~~a~~ diameter of ~6.2 cm were used to estimate snow density. Thus, each snow pit had 2-20 measurements of density, depending on the time available for pit observations to derive bulk density. A table noting survey dates and density methods is available in Appendix B (Table B1). Notes were also taken about qualitative observations of liquid water ~~pooling~~ponding or ice lenses with depth of occurrence and approximate thickness.

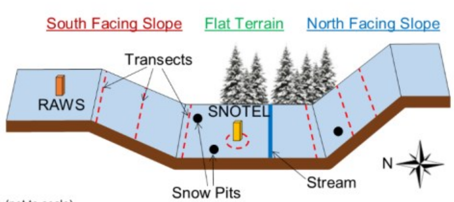

~~Figure 2: Locations of GPR and depth probe transects on the hillslopes of the study area (not to scale).~~

2.3 Data Processing

Radar data for each transect were processed using ReflexW~~ for each transect~~, a software developed for near-surface geophysical data processing and interpretation. The first processing step was to apply a dewow filter, which removes low frequency noise in the time domain by subtracting a running mean from the central point. Applying this filter allows the trace to have a mean of zero which removes any slope in the trace and allows for positive and negative signals throughout the trace. A time-zero correction was applied next by selecting the air wave first break. A gain filter was then applied to account for signal attenuation and geometrical spreading loss as the wave propagates through the snow by amplifying the strength of later arrivals. An AGC-Gain function was used which applies a multiplying factor to successive regions of the trace in time, dampening ~~un-necessary~~ noise. The next step was to edit trace range along the x-axis. This step can be used to remove time periods when the GPR was not moving. During data collection, there are periods of standstill between when the device is powered on and when the transect data are being collected, and between when the transect ends and the device is turned off. Removing the traces before and after effectively crops the radargram to only include the transect data and not oversample the ends of the transect. Finally, a background removal filter is applied. This filter removes any excess noise and excess banding that may be present in the traces. In this step, the processing is set for all data at 1 ns or greater to retain the surface wave, which retains the clarity of the surface wave and soil-snow interface wave during picking. Next, the surface and soil-snow interface reflections were 'picked' using a semi-automatic picking tool in ReflexW. Figure ~~3a~~2a displays an example of a radargram showing the snow surface reflection and snow-soil interface reflection. The surface wave reflection was then subtracted from the snow-soil interface reflection to determine the two-way-travel time (TWT) through the snow (Webb & Mooney, 2024c). Images of all radargrams are available in supplementary material (Figures S1 – S32).

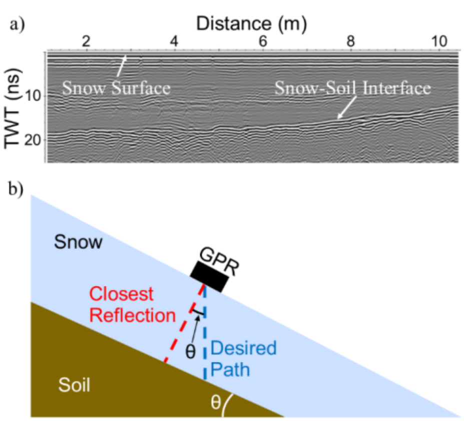

Figure ~~3~~2: a) An example of a processed radargram and the snow surface and snow-soil interface reflections. b) A graphical depiction of the correction for slope angle to align TWT and depth probing for each transect.

The median TWT (ns) for each GPR transect and associated average measured d_s (m) ~~was~~were used for the following calculations to estimate bulk snowpack density~~:~~ by first calculating radar wave velocity (v):

$$\cancel{v = \frac{d_s}{\frac{TWT}{2}}}$$

$$v = \frac{d_s}{\frac{TWT}{2}} \qquad (1)$$

where v is ~~the radar wave velocity~~ in m ns^{-1}, and ~~k_s~~ε is calculated with the speed of light (c) in a vacuum:

$$\cancel{k_s = (\frac{c}{v})^2}$$

~~and bulk density (ρ_s, kg m^{-3}) is estimated using *Kovacs et al.* (1995):~~

$$\cancel{\rho_s = \frac{\sqrt{k_s} - 1}{0.845} * 1000}$$

$$\varepsilon = (\frac{c}{v})^2 \qquad (2)$$

and bulk density (ρ_s, kg m^{-3}) is estimated using *Kovacs et al.* (1995):

$$\rho_s = \frac{\sqrt{\varepsilon} - 1}{0.845} * 1000 \qquad (3)$$

SWE was also calculated by multiplying the estimate of ρ_s by the observed d_s.

When traveling in sloped terrain, the GPR TWT needs to be corrected since a GPR will receive the reflection of the closest reflector that will tend to be normal to the slope. Thus, we adjusted the TWT to be in-line with gravity to ensure the same direction of depth probing by dividing by the cosine of the slope angle (Fig. ~~3b).~~2b). GPR transects were also conducted next to snow pits and the SNOTEL station to calibrate GPR-derived ρ_s estimates for each survey date based on average bias when comparing the transects with an adjacent snow pit or SNOTEL station data.

2.4 Meteorological Data

Hourly data from SNOTEL and RAWS stations in the Dry Lake study site were utilized for the 2023 water year~~. These data are used~~ to contextualize field measurements taken during the observation period and as inputs into a physical snowpack model. ~~Downward longwave radiation was collected for~~The Dry Lake SNOTEL station is centrally located in the ~~area using Hydrology Data Rods, NLDAS Primary Forcing Data (Teng et al., 2016; Xia et al., 2012).~~

Formatted: Line spacing: Double

Formatted: Line spacing: Double

~~The~~watershed in flat terrain at 2521 masl (8271 ft) while the Dry Lake Colorado RAWS station is at 2536 m (8320 ft) elevation on the ridge of the south aspect of the study area~~ while the Dry Lake SNOTEL station is centrally located in the watershed in flat terrain at 2521 m (8271 ft).~~. The ~~RAWS data records include hourly precipitation, wind speed, wind direction, relative humidity, max wind gust speed and direction, and incoming shortwave radiation. The SNOTEL site~~SNOTEL data include hourly measurements of precipitation, SWE, wind speed, air temperature, ~~and~~ snow depth, and soil moisture. Midnight values are quality controlled by snow survey staff to account for error in sensors; however, hourly data is not edited at the time of this study. Using the following rules, hourly data from SNOTEL ~~was~~were corrected to create continuous, hourly data for model input: 1) Accumulated precipitation cannot decrease, 2) If there is an increase in snow depth, there must be an increase in SWE, 3) An increase in SWE should prompt an increase in accumulated precipitation, and 4) Hourly data must fit within the limits of the preceding and following midnight values, but hourly patterns can be preserved. Note that this processing method assumes that wind redistribution and canopy unloading is negligible, which is a reasonable assumption for this SNOTEL station based on observations and distance from any canopy. From these hourly data, ρ_s was calculated for the SNOTEL station by dividing SNOTEL observed SWE by d_s. Physically impossible densities were removed (i.e., negative densities and those greater than the density of water) by replacing those values with the value from previous timestep value. Figure ~~4~~3 displays the processed SNOTEL SWE, cumulative precipitation, d_s, and ρ_s data used for this study. The RAWS data includes hourly precipitation, wind speed, wind direction, relative humidity, max wind gust speed and direction, and incoming shortwave radiation. Downward longwave radiation, necessary for the physical snowpack model, was collected for the area using Hydrology Data Rods, NLDAS Primary Forcing Data (Teng et al., 2016; Xia et al., 2012).

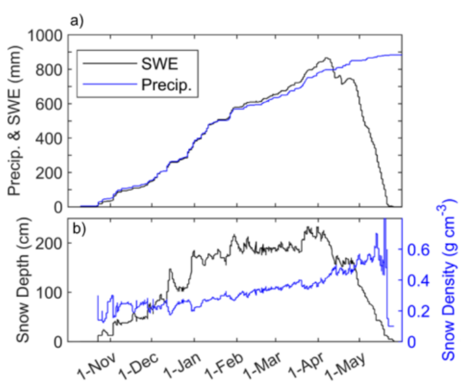

Figure ~~4~~3: SNOTEL data for the ~~2024~~2023 water year showing a) observed SWE and cumulative precipitation, and b) observed snow depth and calculated snow density.

2.~~4~~5 SNOWPACK Modelling

~~The SNOWPACK model (Bartelt and Lehning, 2002) simulates seasonal snowpack based on weather station data. This study uses~~The SNOWPACK model (Bartelt and Lehning, 2002) simulates seasonal snowpack based on weather station data. This study uses SNOWPACK due to past studies validating the liquid water representation in the model structure (e.g., Wever et al., 2014). We used SNOWPACK to represent energy balance changes occurring on each aspect of the watershed to contextualize observations made in the field, with the primary objective of informing the researchers about the timing of snowmelt events. SNOWPACK discretizes the vertical snow profile into multiple layers~~, increasing~~ to account for energy and mass transfer through the accumulation and ~~decreasing through~~ melt ~~and compaction~~phases of the snowpack. In addition to closing the mass and energy balances per time step, the model includes physically-based routines for internal snowpack processes ~~(e.g. liquid water transport and energy exchange) and a unique empirical scheme for snow grain metamorphism.~~. Simulated snow depth, SWE, snowpack temperature, and stratigraphy have been extensively validated for SNOWPACK ~~(Jennings et al., 2018a; Lundy et al., 2001; Meromy et al., 2015; Rutter et al., 2009).~~(Jennings et al., 2018a; Lundy et al., 2001; Meromy et al., 2015; Rutter et al., 2009). SNOWPACK has also been shown as a successful tool in predicting snow liquid water content (LWC) in previous studies ~~(Webb et al., 2018c; Webb et al., 2020a; Webb et al., 2021a).~~(Wever et al., 2014; Würzer et al., 2017; Webb et al., 2021a).

Simulations were run at hourly time steps with quality-controlled observations of air temperature, relative humidity, wind speed, incoming shortwave radiation, incoming longwave radiation, ~~precipitation, and ground surface temperature to simulate the accumulation and melt of a snowpack. The precipitation phase threshold was increased from the default SNOWPACK value of 1.3°C to 2.5°C because the Rocky Mountains of the western United States have some of the highest rain-snow thresholds in the northern Hemisphere (Jennings et al., 2018b). Turbulent energy exchange was simulated using the bulk Richardson number approach as this stability correction produced the best model performance at another subalpine site in Colorado (Jennings et al., 2018a). SNOWPACK simulates the transport of liquid water using Richard's equation (Wever et al., 2014).~~and precipitation to simulate the accumulation and melt of a snowpack. The first simulation represents the flat terrain of the study area using mostly SNOTEL data. The second simulation represents the north aspect hillslope. The third simulation represents the south aspect hillslope near the exposed ridge at the top extent of elevation for the study area, using mostly RAWS station data (which is positioned on the ridge of the south aspect). The precipitation phase threshold was increased from the default SNOWPACK to a value of 2.5°C because the Rocky Mountains of the western United States have some of the highest rain-snow thresholds in the northern Hemisphere (Jennings et al., 2018b). Turbulent energy exchange was simulated using the bulk Richardson number approach as this stability correction produced the best model performance at another subalpine site in Colorado (Jennings et al., 2018a). We did not define soil layers in SNOWPACK simulations because the primary focus of the modelling component is to inform us of the timing of snowmelt events. Additionally, canopy was not considered in our modelling to represent general conditions for each terrain condition. Further details on parameter decisions for the SNOWPACK simulations are offered in Appendix C.

~~The first model is a south facing exposed ridge at the top extent of elevation for the study area, using mostly RAWS station data (which is positioned on the ridge of the south aspect). The second model represents the flat terrain of the study area using mostly SNOTEL data. The third location modelled is on the north aspect. The north aspect and south aspect models do not consider canopy effects to represent general hillslope conditions.~~

3. Results

3.1 Transect Data

~~We found transects in~~For the ~~flat terrain transects show snow depth and SWE increasing during~~2023 water year the ~~accumulation period similar to SNOTEL data, January through April.~~ SNOTEL peak SWE ~~occurs~~occurred on April 6 at 866 mm, followed by rapid decreases in snow depth and SWE. We found the flat terrain transect observations followed similar snow depth and SWE patterns as SNOTEL data. In this ~~region~~location, transect data showed similar peak snow depth, but slightly lower SWE and ρ_s values during the 1~~-~~ Apr survey (Fig. ~~5d~~4a). In general, the flat terrain transect data compared well with SNOTEL data.

Snow depth on the north aspect follows a similar pattern to the flat terrain with increases during the accumulation phase and a rapid decrease starting in April~~,~~ (Fig. 4b-d), though this period also resulted in large increases in ρ_s indicating an increased rate of densification while SWE increases slightly. North aspect d_s values are highest overall with the top of slope consistently producing the deepest snow throughout the season (Fig. ~~5g~~4b). However, we observed two distinct patterns in ρ_s on the north aspect. The first pattern is for the top and middle of the north aspect slope showing a relatively consistent ρ_s through the early surveys, and a large increase of ρ_s for the May survey (Fig. ~~5f-g~~4b-c). The second pattern occurred at the base of slope showing a consistent increase from February to April. This base of the north aspect also resulted in an unrealistic value during the May survey (Fig. 4d) that we interpret as being the result of excessive liquid water content due to a very low radar velocity and high relative dielectric permittivity ~~(Bradford et al., 2009; Webb et al., 2018c). The SWE estimates from transect data follows these same ρ_s patterns on the north aspect.~~ (e.g., Bradford et al., 2009). This location has also been previously observed to result in excessive liquid water during spring snowmelt (Webb et al., 2018a), though no snow pit was dug at this location in May for the 2023 water year.

~~The~~We found the south aspect transects had ~~different~~unique patterns relative to the flat terrain and north aspect during both the accumulation and melt phases of the snowpack (Fig. ~~5~~4). The d_s at the top and middle position of the south aspect show gradual increases from January to April, with both gains and losses in SWE during this time (Fig. ~~4a-b~~4e-f). The base of the south aspect sees a similar pattern of increasing depth, but with SWE consistently increasing from January through April surveys (Fig. ~~5e~~4g). All transects on the south aspect experienced a decline in SWE from the April to May surveys, though the smallest change occurs at the base of the south aspect, coinciding with a large increase in ρ_s at this location (Fig. ~~5a-c~~4e-g).

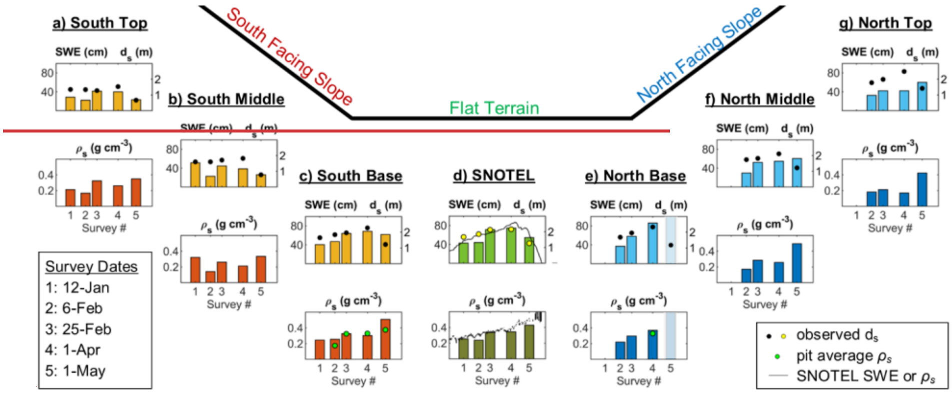

Qualitative observations were also noted during transect surveys including surface melt on the south aspect forming small runnels in the afternoon during the 1 April survey. While wet snow was qualitatively observed in snow pits on other aspects as well, the south aspect was the only location that was observed to pond on layers and form snow surface runnels. We interpret this to indicate that the south aspect slope transports some liquid water laterally through the snowpack at times when other areas of the watershed are not. Additionally, soil moisture sensors at the SNOTEL station show a steady rise in soil moisture through snow accumulation, indicating a steady source of moisture throughout the winter (Fig. 5).

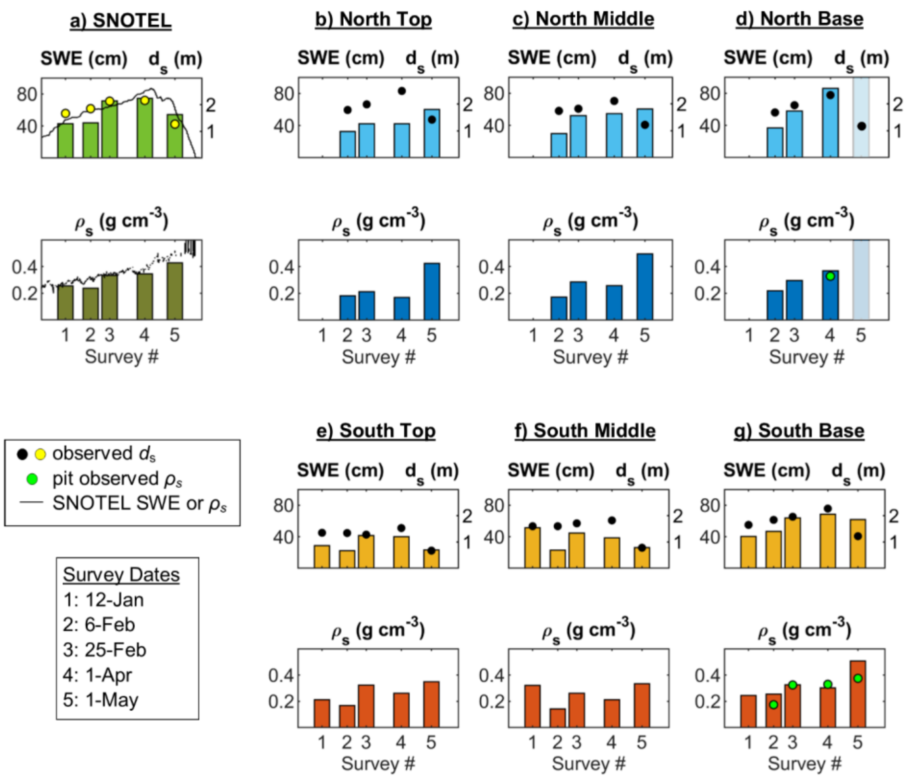

Figure ~~5~~4: Results from the transect observations including calculated SWE, observed d_s, and GPR derived ρ_s for: a) ~~South Top, b) South Middle, c) South Base, d)~~ Flat Terrain around the SNOTEL station, ~~e~~b) North ~~Base, f~~Top, c) North Middle, d) North Base, e) South Top, f) South Middle, and g) ~~North Top~~South Base locations. Pit measured average densities are shown when collected, and SNOTEL station data are displayed for additional comparisons of SWE and ρ_s. Note that the GPR results that gave unrealistic values due to the presence of liquid water is slightly greyed in panel ~~e~~d.

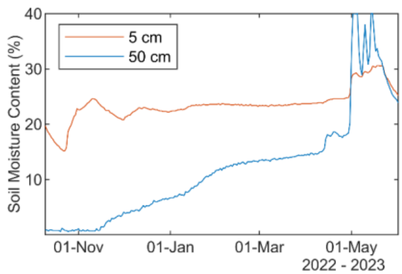

Figure 5: Soil moisture data from the SNOTEL site at depths of 5 cm and 50 cm.

3.2 Snow Pit Observations

In general, the snow pits show patterns of increasing density with depth and time, as expected, with ice lenses and layers forming from the upper to mid snowpack in all pit locations (Fig. ~~6). Pits dug at the base of the south aspect showed a single ice layer during the 28 Febrary and 1 April surveys.~~ 7~~This ice layer was approximately 4 cm thick at ~150 cm above ground in February and approximately 11 cm thick ~70 cm above ground in April (Fig. 6~~a). The flat terrain pit did not have any ice lenses/layers in January, but one ice lens was observed in April that was approximately 3 cm thick and ~230 cm above the ground (Fig. ~~6b~~7a). The north aspect only had a single snow pit observation during the 1 April survey, but ten ice lenses/layers were observed throughout the snowpack from 30 cm to 210 cm above the ground, all were approximately 1-2 cm thick (Fig. 7b). Seven of the ten observed ice lenses/layers were observed within a 70 cm section of the pit, from 110 – 180 cm above the ground (240 cm total pit depth). Pits dug at the base of the south aspect showed a single ice layer during the 28 February and 1 April surveys. This ice layer was approximately 4 cm thick at ~150 cm above ground in February and approximately 11 cm thick ~70 cm above ground in April (Fig. ~~6c).~~7c).

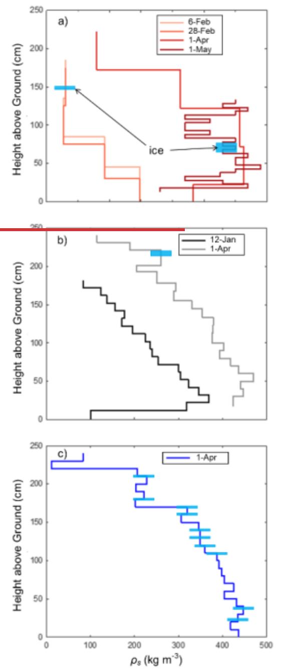
a)
6-Feb
28-Feb
1-Apr
1-May
ice
Height above Ground (cm)
b)
12-Jan
1-Apr
Height above Ground (cm)
c)
1-Apr
Height above Ground (cm)
ρs (kg m-3)

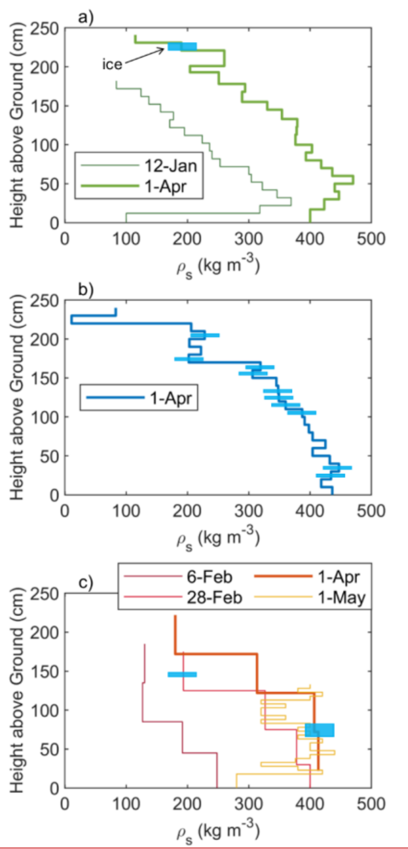

Figure 6: Snow pit observations of ρ_s and ice layers/lenses for: a) flat terrain, b) north aspect, and c) the base of the south aspect~~, b) flat terrain, and c) north aspect~~. We estimate an uncertainty of approximately 10% for these density measurements.

3.3 SNOWPACK Modelling Results

Modelling of d_s, ρ_s, SWE, and ~~SWE~~snow LWC were completed using the SNOWPACK model to simulate accumulation and melt on the flat terrain, north aspect, and south aspect~~, and flat terrain~~ areas of the study site. ~~The north aspect model indicates the largest snow depths and longest snow persistence, as expected due to terrain shading (Fig. 7a-b).~~ The flat terrain ~~model~~

~~produces a model~~simulation produced results matching the SNOTEL data well during accumulation, but with slightly different melt rates in May~~ (Fig. 7a-b).~~. The north aspect simulation resulted in the largest snow depths and longest snow persistence (Fig. 7a-b). The south aspect ~~model shows~~simulation showed the lowest snow depth and the earliest melt out date. ~~(Fig. 7a-b).~~ The simulated ρ_s ~~modelled~~ in SNOWPACK is similar across each aspect until April when melt begins. SNOWPACK simulated bulk ρ_s showed a root mean squared error of 48 kg m^{-3} when compared to pit observed ρ_s. During the first two surveys (12 Jan and 6 Feb) SNOWPACK overestimated ρ_s whereas it underestimated ρ_s during the late February and May surveys (28 Feb and 1 May). SNOWPACK simulated ρ_s was within 10 kg m^{-3} of pit observed ρ_s for all three pits on 1 Apr, representing a bias of less than 2% near peak SWE. All model simulations indicate a spike in density prior to completely melting out, but with different amplitudes and timing. The ~~modelled~~simulated SWE shows similar patterns relative to SNOTEL data. ~~The north aspect model accumulates more snow than the SNOTEL data, as expected. Peak SWE in the north aspect model occurred on April 24 at ~920 mm, whereas~~ SWE peaks in both the flat and south aspect ~~models~~simulations on 5 April~~ 5~~ (~810 mm and ~285 mm, respectively), the date of a snowstorm prior to a period of warmer weather~~.~~, whereas peak SWE in the north aspect model occurred on April 24 at ~920 mm. In comparing the SNOWPACK simulated SWE to GPR estimated SWE near simulated peak SWE dates, we see the flat terrain had an estimated 744 mm from GPR (833 mm from SNOTEL pillow) compared to simulated 786 mm for 1 Apr (~5% difference), the north aspect slope had an estimated 603 mm compared to a simulated 813 mm (~35% difference), and the south aspect slope had an estimated 392 mm compared to the simulated 265 mm simulated for 1 Apr (~33% difference). The SNOWPACK simulation captures the increase and decrease in SWE relative to north and south aspect, respectively, with similar magnitude differences compared to transect estimates of SWE near peak SWE.

All ~~model~~SNOWPACK simulations show intermittent surface melt events (Fig. 7c-d), with the largest and most regular occurring on the south aspect simulation (Fig. 7e). ~~Simulated bulk volumetric LWC on the south aspect increases to 1% or more nine times from December through March (Fig. 7e).~~ The ~~other~~ flat terrain and north aspect ~~and flat terrain model~~ simulations ~~do~~did not ~~see~~result in volumetric LWC values greater than 0.5% for ~~that same~~the period of December through March (Fig. 7c-d). However, south aspect simulated bulk volumetric LWC increases to 1% or more nine times from December through March (Fig. 7e). Additionally, simulated LWC at the base of the snowpack, indicating timing of simulated snowmelt runoff, occurs only during the early accumulation season and after peak SWE for all simulations (Fig. 7c-e).

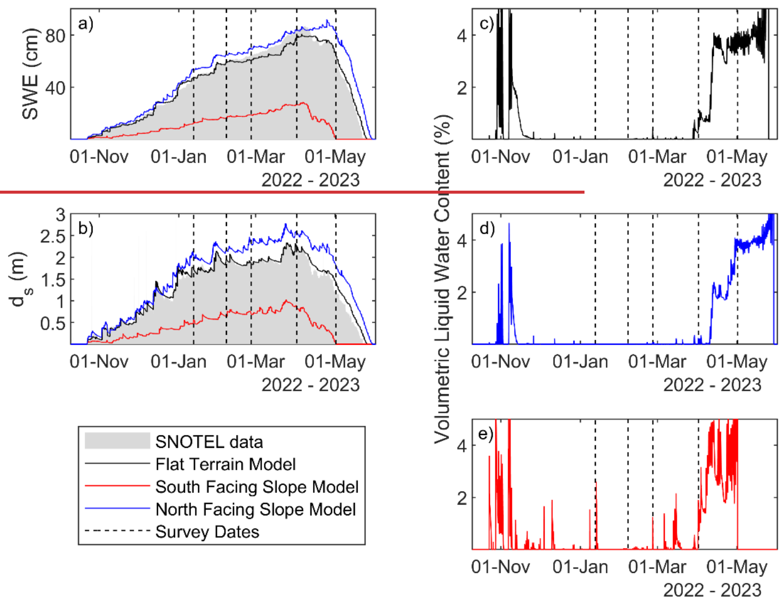
a)
SWE (cm)
80
40
01-Nov
01-Jan
01-Mar
01-May
2022 - 2023
b)
d_s (m)
3
2.5
2
1.5
1
0.5
01-Nov
01-Jan
01-Mar
01-May
2022 - 2023
SNOTEL data
Flat Terrain Model
South Facing Slope Model
North Facing Slope Model
Survey Dates
Volumetric Liquid Water Content (%)
c)
4
2
01-Nov
01-Jan
01-Mar
01-May
2022 - 2023
d)
4
2
01-Nov
01-Jan
01-Mar
01-May
2022 - 2023
e)
4
2
01-Nov
01-Jan
01-Mar
01-May
2022 - 2023

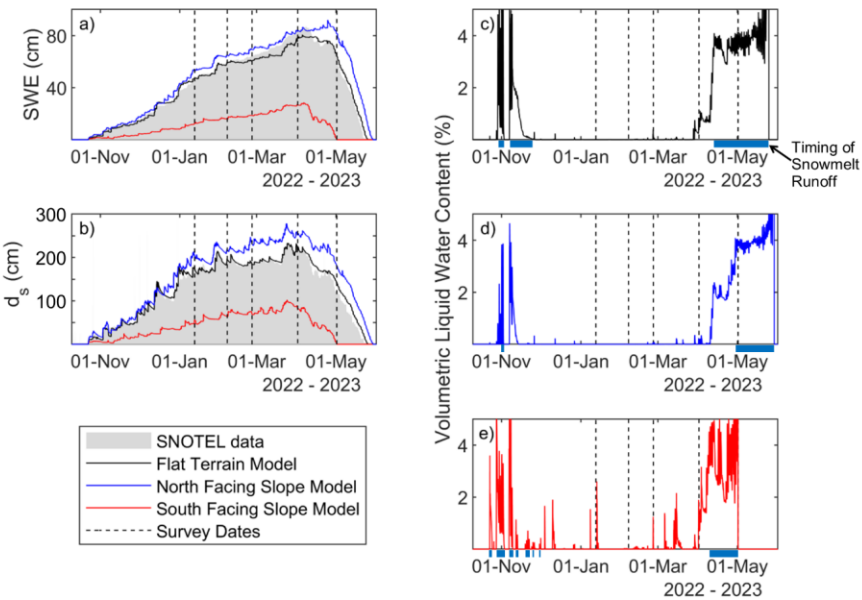

Figure 7: Results from the SNOWPACK ~~model~~ simulations including a) SWE, b) d_s, and c) – e) volumetric liquid water content. Panels c) – e) also show when simulated snowmelt runoff from the snowpack is occurring as blue bars. Results show comparison to SNOTEL data as well as timing with survey dates.

4. Discussion

This study observed snow density variation with aspect and position on slope using pit calibrated GPR transects. The results ~~show mid-season melt occurring on the south aspect~~ showed flat terrain transect data that ~~redistributes SWE down towards the base of the slope,~~matched well with SNOTEL d_s and ~~pooling~~SWE measurements (Fig. 4). The flat terrain SNOWPACK simulation results also matched well with observational data from the SNOTEL station as well as survey transect data (Fig. 7). SWE varied slightly from the measured to the simulated data, likely due to precipitation uncertainties relative to snow on the ground as observed by the snow pillow. The results of this study also suggests ponding of LWC in the snowpack at the base of the north aspect during the ripening and melt phase whereas mid-season surface melt occurring on the south aspect hillslope is interpreted as redistributing SWE down towards the base of the slope. Variation in snow depth and density along both hillslopes have implications for SWE distribution and peak timing, indicating the importance of aspect-specific considerations for modelling of SWE and melt processes ~~(Sexstone and Fassnacht, 2014; Lopez-Moreno et al., 2013).~~(Sexstone and Fassnacht, 2014; Lopez-Moreno et al., 2013).

~~The flat terrain area did not produce any unusual results. GPR values matched well with SNOTEL d_s and SWE measurements (Fig. 5). The flat terrain SNOWPACK model also showed results that matched well with observational data (Fig. 7). SWE varied slightly from the measured to the modelled data, likely due to precipitation uncertainties relative to snow on the ground as observed by the snow pillow.~~

4.1 Uncertainty Estimation of Survey Data

The above-described methods in estimating ρ_s through manual depth probes and GPR will include uncertainty from both data sources. The manually measured d_s data are estimated to have an average uncertainty of 3% for the transect area for an average of 13 measurements (Lopez-Moreno et al., 2011), while the GPR TWT will have an uncertainty that is approximately equal to 0.25 of the wavelength, or 0.25 ns for 1000 MHz (Burger et al., 2006). It is important to note that both of these uncertainty estimates are conservative and the true uncertainty is likely lower, though these estimates provide a quantitative measure of maximum uncertainty for our ρ_s estimates. These estimates result in relative uncertainty for radar v of 3.1% that propagates to ρ_s estimates that averaged approximately 17% (~45 kg m^{-3}) that is driven predominantly by d_s uncertainty. These are similar results to other studies pointing towards snow depth being the greatest source of uncertainty when using equation (3) (McGrath et al., 2022), though higher than other studies using LiDAR for snow depth (Meehan et al., 2024). Further details of uncertainty calculations are provided in Appendix D.

The estimated uncertainty of ~45 kg m^{-3} is similar in magnitude to the mean bias of 48 kg m^{-3} (mean absolute deviation of 60 kg m^{-3}) of the transect ρ_s estimates relative to snow pit and SNOTEL data. This direct comparison was used for calibration due to the observation of liquid water being present in snow pit observations during surveys, indicating that the relative uncertainty of using equations (1), (2), and (3) is likely lower than the above estimate for dry snow conditions along the transects of this study. After calibrating the transect ρ_s estimates to snow pit and SNOTEL data, the mean error was less than 5 kg m^{-3} (mean absolute deviation of 45 kg m^{-3}).

4.2 Limitations of Study

It is important to also discuss the limitations of the present study and potential ways to overcome these in future studies. The SNOWPACK simulations used could be further calibrated. In future studies the use of a multi-dimensional model could also be beneficial to further consider the influence of forest canopy and wind transport, factors that have been found to be just as important as aspect (Mazzotti et al., 2023). However, there is not currently a hydrologic model that incorporates lateral flow through snow, so more snow pits along with quantitative observations of LWC and lateral flow processes could further our understanding (e.g., Thompson et al., 2016). The use of sensors installed within a snowpack could also provide further time-series data (e.g., Díaz et al., 2017) to observe the presence and ponding of liquid water at locations of interest. These observations could provide more precise observations rather than the bulk estimates using the methods in the present study.

4.3 Perceptual Model

Northern hemisphere incidence angle of the sun allows for more exposure on the south aspect compared to the north aspect, which is shaded more of the time. This influences the energy balance of the snowpack by reducing energy inputs to the north aspect and increasing energy inputs to the south aspect, resulting in differences in accumulation and melt dynamics ~~(Molotch and Meromy, 2014; Erickson et al., 2005).~~(Molotch and Meromy, 2014; Erickson et al., 2005). Additionally, the south aspect ~~doesn't~~does not receive canopy shading in the winter because it is canopy free in the top half of slope and is populated with deciduous Aspen on the lower half of slope, which lose their canopy during the winter ~~(Musselman et al., 2008; Varhola et al., 2010).~~(Musselman et al., 2008; Varhola et al., 2010). There is some coniferous canopy on the north aspect slope, though the canopy is denser at the base of the slope. This difference in canopy cover is likely attributed to aspect as the deeper snow and increased soil moisture on the northern aspect increases the amount of plant available water for vegetation growth (Webb et al., 2023). However, transects were selected to have minimal canopy influence for hillslope observations, though this could not be accomplished at the base of the north aspect that did have some canopy shading.

The north aspect is an area of lower solar radiation exposure resulting in greater snow depths and later melt throughout the winter and spring seasons relative to other locations observed for this study. The north aspect hillslope is partially forested as well, which is likely a result of terrain shading and greater water availability during the growing season. This coniferous canopy remains intact throughout the winter months, providing shelter from wind and solar radiation, allowing snow to accumulate and persist longer. The survey transect higher up on the north aspect resulted in greater depths. Further down at the middle of the slope, depth decreases slightly with minimal SWE differences relative to the top of the slope. The transect in the middle of the north aspect has partial canopy coverage with parts near the drip edge of trees that likely resulted in some interception but also canopy sloughing that caused the lower depths and higher densities at this location relative to the top of the north aspect. The base of the north aspect is in a small opening of the mostly forested location of this study, though interception did not cause a large difference in accumulated snow depth ~~(Webb et al., 2023). This increased exposure on the south aspect results~~(Fig. 4e). The most notable difference at the base of the north aspect is the steady increase in snow density through the observation period, with an unrealistic increase in ρ_s during the May survey (ρ_s > 1000 kg m^{-3}). Once the snowpack begins to ripen, ρ_s spikes to values that are not physically possible, which is indicated by the GPR signal slowing, likely from liquid water in the snowpack. This could be a result of the exposed areas of the slope producing meltwater which flows downhill and ponds at the base of the slope as previously observed at this site (Webb et al., 2018a). Unlike the south aspect, here on the north aspect most of the SWE has remained on the hillslope through the winter, rather than melting intermittently with mid-season melt events. This excess of water on the north aspect slope, paired with fine-grained soils with low infiltration capability, could explain ponding of liquid water at the base occurring with the onset of the melt phase. Snow pits dug on 1 April at the base of slope further support this interpretation, as several ice lenses/layers distributed throughout the snowpack were observed indicating the presence of multiple hydraulic barriers with the potential to divert liquid water laterally in the snowpack the entire length of the hill slope (Eiriksson et al., 2013; Webb et al., 2018b).

The increased exposure on the south aspect resulted in SWE losses from three mechanisms: melt, sublimation, and wind scouring. Wind sensors on the RAWS station indicate that windspeeds top out at 6-10 m/s with most gusts ~~traveling~~coming from the northeast. The precipitation at this ridgeline sensor is lower compared to the SNOTEL sensors in the flats, likely ~~indicating strong~~a result of stronger winds blowing snow over the gauge. These kinds of wind could contribute to scouring of snow. Blowing snow is also more susceptible to sublimation ~~(Vionnet et al., 2013).~~(Vionnet et al., 2013). Modelling of snow depth and SWE on the south aspect are largely a product of precipitation input from RAWS data, resulting in lower values compared to measurements (Fig. 7). Melt out dates reflect these lower precipitation inputs as well, with observable snow depth surveyed on 1 May ~~1st~~ while the model simulated this as the last day of snow cover for the south aspect (Fig. 7). Despite model ~~weaknesses, the~~differences in melt out dates, the simulated LWC parameter shows when surface melt occurred due to its root in physical processes~~.~~ and qualitative comparison to snow pit observations. The south aspect ~~model~~simulation reveals several mid-season surface melt events that are not present in the flat or north aspect models, which is likely a response to increased solar radiation exposure that were also qualitatively observed during surveys. These mid-winter melt events on the south aspect coincide with increased density at the base of slope~~, indicating a likely downhill migration of SWE through intra-snowpack flowpaths (Webb et al., 2020a; Webb et al., 2022). There is also the observation of an ice layer at the base of the south aspect that is indicative of lateral flow in sloping terrain (Webb et al., 2018b).~~ (Fig. 4) and the formation and thickening of an observed ice lense (Fig. 6), that we are interpreting as an indication of likely downhill migration of SWE through intra-snowpack flowpaths (Webb et al., 2020a; Webb et al., 2022; Eiriksson et al., 2013). The ice layer observed at the base of the south aspect is indicative of lateral flow in sloping terrain (Webb et al., 2018b; Schlumpf et al., 2024) as it is likely thick enough at 7 cm to create an hydraulic barrier and promote lateral flow. Observations of surface melt occurring on the south aspect also included small runnels forming late in the afternoon during the April survey, which is further supporting this interpretation. Additionally, soil moisture sensors at the SNOTEL station indicate a steady rise in soil moisture that align with snowpack accumulation, indicating a steady source of moisture throughout the winter (Fig. ~~8~~5). With lateral groundwater fluxes from outside this watershed assumed to be ~~minimal~~negligible, the source of soil moisture rise is likely from melting snow on the south aspect as snow elsewhere in the watershed remains cold enough to not provide moisture inputs~~.~~ (Supplementary Tables S1-S7). These results indicate the input of snowmelt from the south aspect may be providing connectivity to the stream and water sources to potentially maintain baseflow through the winter, though streamflow data are not available for this location~~ and requires further research in the future.~~. Further quantification of subsurface properties such as porosity and saturation of soils on the slope could clarify these processes and fully describe vadose zone hydrologic connectivity and water movement.

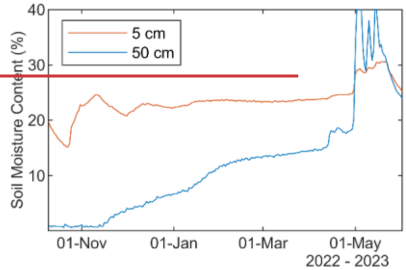

~~**Figure 8: Soil moisture data from the SNOTEL site at depths of 5 cm and 50 cm.**~~

~~The north aspect is an area of lower solar radiation exposure compared to the south aspect. This is evidenced by greater snow depths and later melt throughout the winter and spring seasons. The region is partially forested as well, which is likely a result of terrain shading and greater water availability during the growing season . This coniferous canopy remains intact throughout the winter months, providing shelter from wind and solar radiation, allowing snow to accumulate and persist longer. The survey transect higher up on the north aspect resulted in greater depths as a result of low canopy interception. Further down at the middle of the slope, depth decreases slightly with minimal SWE differences relative to the top of the slope. The transect in the middle of the north aspect has partial canopy coverage with parts near the drip edge of trees that likely resulted in some interception but also canopy sloughing that caused the lower depths and higher densities at this location relative to the top of the north aspect. The base of the north aspect is in a small opening of the mostly forested location of this study, though interception did not cause a large difference in accumulated snow depth Fig. 5e). The most notable difference at the base of the north aspect is the steady increase in snow density through the observation period, with an unrealistic increase in density during the May survey. Once the snowpack begins to ripen, density spikes to values that are not physically possible, which is an indication of GPR signal slowing from liquid water in the snowpack. This could be a result of the exposed areas of the slope producing meltwater which flows downhill and pools at the base of the slope as previously observed at this site (Webb et al., 2018a). Unlike the south aspect, most of the SWE has remained on the hill, rather than melting intermittently with mid-season melt events. This excess of water, paired with fine-grained soils with low infiltration capability, could explain pooling of liquid water at the base occurring with the onset of the melt phase. Snow pits dug on April 1st at the base of slope further support this interpretation, as several ice lenses/layers distributed throughout the snowpack were observed indicating multiple hydraulic barriers with the potential to divert liquid water laterally in the snowpack the entire length of the hill slope (Webb et al., 2018b).~~

The energy balance proved to have a large effect on field data and modelling as the south aspect ~~model~~simulations encompassed greater energy inputs and exposure than the north-aspect, resulting in different accumulation and melt dynamics. While these specific basin dynamics are not applicable to every snowpack, there are some general patterns that can be applied to areas with similar characteristics. For instance: 1) ~~Open canopy, south aspects have greater potential for mid-winter melt events, causing a redistribution of SWE downslope to increase SWE and soil moisture (Fig. 9a); and 2)~~ north aspects in this type of environment may experience lateral flow of water through snow and in the shallow subsurface causing accumulation and ~~pooling of liquid water at the base of slope during spring ripening and snowmelt (Fig. 9b; Webb et al., 2018a). Figure 9 offers an update to the *Webb et al*. (2018a) conceptual model of~~ponding of liquid water at the base of slope during spring ripening and snowmelt (Fig. 8b; Webb et al., 2018a); and 2) open canopy, south aspects that develop a seasonally persistent snowpack have greater potential for mid-winter melt events, interpreted in this study to cause a redistribution of SWE through liquid water transport downslope, increasing SWE and soil moisture (Fig. 8a). Figure 8 offers an update to the *Webb et al*. (2018a) perceptual model of these aspect controls on liquid water movement, with descriptions of the dominant processes during the winter and spring periods. Canopy and wind drifting influences are not interpreted as major contributions to the redistribution of SWE at Dry Lake due to the wind direction being parallel to the study slope contours and observations of drifting not occurring at our transect locations. However, some canopy shading will influence the observations at the base of the north aspect hillslope though terrain shading dominates the energy balance as previously mentioned. Thus, we interpret the lateral flow of liquid water to be a major factor in the redistribution of SWE as presented in the perceptual model for the Dry Lake site (Fig. 8).

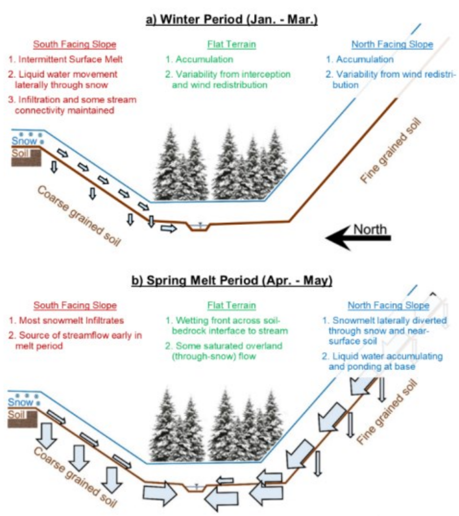

Figure 8: Perceptual model of interpretation of processes during a) the winter period (January through March) and b) spring melt period (April through May). Panel (b) is modified from Webb et al. (2018a).

The main objective of this study was to determine how SWE and snow density ~~changes~~change with aspect and position on hillslope. We found that sloped areas can have quite different melt dynamics which can greatly influence snow density. In particular, the base of slope seemed to be an area of greater SWE following different melt mechanisms (Fig. ~~9~~8). Each aspect melts at different times because of varying energy balance dynamics. ~~The south aspect is responding to mid-winter melt, which is distributing mass to the base of slope during the middle of the winter whereas the~~The north aspect ~~is experiencing~~experiences primarily accumulation during winter and distribution of mass through melt processes during the spring ripening and snowmelt periods in April whereas the south aspect is responding to mid-winter melt, which is distributing mass to the base of slope during this time.

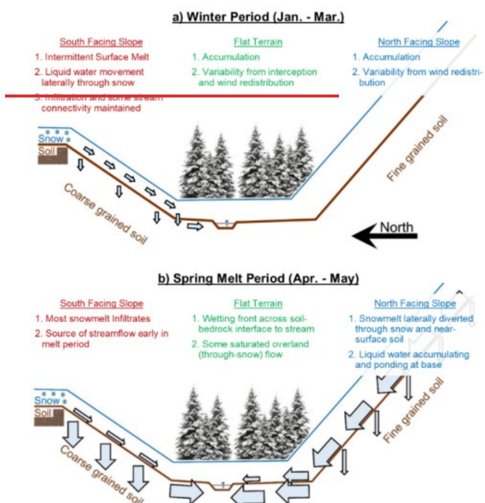

~~**Figure 9: Summary of processes during a) the winter period (January through March) and b) spring melt period (April through May). Panel (b) is modified from Webb et al. (2018).**~~

Assessing patterns in snow density and the influence of the movement of liquid water throughout a watershed and snow season can provide important context to measuring and modelling snow ~~(Webb et al., 2022).~~(Webb et al., 2022). Snowmelt and catchment liquid water input into a system have historically been associated with snowmelt rates; however, snowmelt rates are dependent on complex energy balance interactions between the snowpack and its environment. The traditional 4-phase snowpack model ~~(Dingman, 2015)~~of a homogenous snowpack going through accumulation, warming, ripening, and melt (Dingman, 2015) may not be representative for all snowpacks everywhere in a single watershed at a given time, especially when considering hillslope processes. Position on slope, aspect, and snowpack phases were found to be factors ~~in predicting~~for snow density and presence of liquid water. Areas with higher energy input may see a greater range of density and more dynamic snowpack conditions. Paired with well-known depth variation, these parameters could have a compounding effect on SWE, further emphasizing the importance of quantifying spatial variability of density at the catchment scale. Importantly, other studies have found that canopy structure and weather can be just as important as the topography component focused on in this study (Mazzotti et al., 2023). These results support further quantification of catchment scale density for measurement of SWE, especially on different aspects as they have a significant influence on snowpack energy balance. Similar studies are needed to further understand density variation in systems with different energy balance dynamics, or ~~conversely,~~ future projections of energy balance scenarios.

5. Conclusions

This study found that aspect produces snowpack melt and SWE distribution dynamics that are different from a traditional flat area ~~conceptual~~one-dimensional perceptual model. In general, there is a pattern of downhill SWE migration and densification at the base of either hillslope which is largely influenced by energy input timing. ~~Of these, the~~Of these, the north aspect behaved more like the flat areas during the accumulation phase, with a large change at the onset of April melt interpreted to cause liquid water ponding at the base of the hillslope. The south aspect was found to be susceptible to mid-season melt events which increased snow density that we interpret is occurring through the redistribution of SWE via the lateral flow of liquid water to the base of the hillslope. ~~The north aspect behaved more like the flat areas during the accumulation phase, with a large change at the onset of April melt causing liquid water pooling at the base of the hillslope.~~ These differences between aspects are most related to solar radiation inputs ~~and preferential terrain shading~~.

Appendix A

In this appendix, we present the wind rose produced for the observed winter and snowmelt season at the RAWS station (Fig. A1).

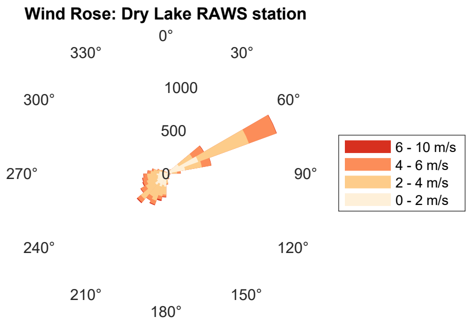

Figure A1. Wind rose for the Dry Lake RAWS site.

Appendix B

In this appendix, we present the density methods that were used for each of the surveys (Table B1).

Table B1. Date and density measurement methods for each of the snow surveys.

Date	Density Method (pit location)
12 Jan	1000 cc wedge cutter (Flat terrain)
6 Feb	50 cm long cores (base of South aspect)
28 Feb	50 cm long cores (base of South aspect
1 Apr	1000 cc wedge cutter (Flat & North aspect) 50 cm long cores (base of South aspect)
1 May	250 cc wedge cutter (base of South aspect)

Appendix C

In this appendix, we provide further details of the SNOWPACK simulation parameterizations. We provide details in the tables below that describe common data sources and modelling decisions for all simulations (Table C1) as well as data sources and model decisions for the south aspect simulation (Table C2), flat aspect simulation (Table C3), and north aspect simulation (Table C4). If a parameter is not listed in the tables, then the default choice in SNOWPACK was used.

Table C1. Data sources and model decisions that are common to all SNOWPACK model simulations in this study.

Variable/Parameter	Data Source/Model Input
Air Temperature	SNOTEL
Relative Humidity	RAWS
Incoming Longwave Radiation	NLDAS
Ground Surface Temperature	0.0 °C
Number of Solutes	0
Roughness Length	0.01
Height of Meteo. Values	4.0 m
Shortwave Mode	Incoming
Atmospheric Stability	Richardson
Canopy	False
Measured Surface Temperature	False
Soil Layers	False
Snow Grooming	False
Research	True
Adjust Height of Meteo. Values	True
Adjust Height of Wind Value	True
Snow Erosion	False
Wind Scaling Factor	1.0
Allow Adaptive Timestepping	True
Rain Threshold	2.5 °C
Water Transport Model	Bucket

Table C2. Data sources and model decisions that were used for the flat aspect SNOWPACK model simulations in this study. Note that the shortwave radiation parameter includes the data source and multiplication factor discussed in the main text.

Variable/Parameter	Data Source/Model Input
Wind Speed	SNOTEL
Height of Wind Value	4.0 m
Shortwave Radiation	RAWS * 1.03
Precipitation	SNOTEL
Enforce Measured Snow Heights	True

Snow Height	SNOTEL

Table C3. Data sources and model decisions that were used for the north aspect SNOWPACK model simulations in this study. Note that the shortwave radiation parameter includes the data source and multiplication factor discussed in the main text.

Variable/Parameter	**Data Source/Model Input**
Wind Speed	RAWS
Height of Wind Value	3.0 m
Shortwave Radiation	RAWS * 0.76
Precipitation	SNOTEL
Enforce Measured Snow Heights	False

Table C4. Data sources and model decisions that were used for the south aspect SNOWPACK model simulations in this study. Note that the shortwave radiation parameter includes the data source and multiplication factor discussed in the main text.

Variable/Parameter	**Data Source/Model Input**
Wind Speed	RAWS
Height of Wind Value	3.0 m
Shortwave Radiation	RAWS * 1.1
Precipitation	RAWS
Enforce Measured Snow Heights	False

Appendix D

In this appendix, we describe the methods used for the uncertainty analysis. We estimate the relative error for equation (1) using the following calculation:

$$\epsilon_v = \sqrt{\epsilon_{TWT}^2 + \epsilon_{d_s}^2} \quad \text{(D1)}$$

where ϵ_i is the percent error associated with parameter *i*. We then propagate this relative error through equations (2) and (3) for estimating permittivity and snow density, respectively, to determine final propagated relative uncertainty.

Data Availability

SNOTEL data are available from the online repository (https://wcc.sc.egov.usda.gov/nwcc/site?sitenum=457) and RAWS data are available through the DRI data repository (https://raws.dri.edu/cgi-bin/rawMAIN.pl?coCDRY). Field survey data are available in the Dry Lake Watershed collection in CUAHSI Hydroshare (Webb, 2024; http://www.hydroshare.org/resource/4aff38a0cbb24456be4e99987e808abb).

Competing Interests

The contact author has declared that none of the authors has any competing interests.

References

~~Bales, R. C., Molotch, N. P., Painter, T. H., Dettinger, M. D., Rice, R., and Dozier, J.: Mountain hydrology of the western United States, Water Resources Research, 42, W08432, 10.1029/2005wr004387, 2006.~~

~~Bartelt, P. and Lehning, M.: A physical SNOWPACK model for the Swiss avalanche warning Part I: numerical model, Cold Regions Science and Technology, 35, 123-145, 10.1016/S0165-232X(02)00074-5, 2002.~~

~~Bishay, K., Bjarke, N. R., Modi, P., Pflug, J. M., and Livneh, B.: Can Remotely Sensed Snow Disappearance Explain Seasonal Water Supply?, Water, 15, ARTN 1147 10.3390/w15061147, 2023.~~

~~Bonnell, R., McGrath, D., Williams, K., Webb, R., Fassnacht, S. R., and Marshall, H.-P.: Spatiotemporal Variations in Liquid Water Content in a Seasonal Snowpack: Implications for Radar Remote Sensing, Remote Sensing, 13, 4223, 2021.~~

~~Bradford, J., Harper, J., and Brown, J.: Complex dielectric permittivity measurements from ground-penetrating radar data to estimate snow liquid water content in the pendular regime, Water Resources Research, 45, 10.1029/2008WR007341, 2009.~~

~~Brooks, P. D., Gelderloos, A., Wolf, M. A., Jamison, L. R., Strong, C., Solomon, D. K., Bowen, G. J., Burian, S., Tai, X., Arens, S., Briefer, L., Kirkham, T., and Stewart, J.: Groundwater-Mediated Memory of Past Climate Controls Water Yield in Snowmelt-Dominated Catchments, Water Resources Research, 57, e2021WR030605, https://doi.org/10.1029/2021WR030605, 2021.~~

~~Clark, M., Hendrikx, J., Slater, A., Kavetski, D., Anderson, B., Cullen, N., Kerr, T., Hreinsson, E., and Woods, R.: Representing spatial variability of snow water equivalent in hydrologic and land-surface models: A review, Water Resources Research, 47, 10.1029/2011WR010745, 2011.~~

~~Clark, M., Fan, Y., Lawrence, D., Adam, J., Bolster, D., Gochis, D., Hooper, R., Kumar, M., Leung, L., Mackay, D., Maxwell, R., Shen, C., Swenson, S., and Zeng, X.: Improving the representation of hydrologic processes in Earth System Models, Water Resources Research, 51, 5929-5956, 10.1002/2015WR017096, 2015.~~

~~Clow, D. W.: Changes in the Timing of Snowmelt and Streamflow in Colorado: A Response to Recent Warming, Journal of Climate, 23, 2293-2306, 10.1175/2009jcli2951.1, 2010.~~

~~Co, M.: Colorado Hazard Mapping: LiDAR [dataset], 2016.~~

~~Currier, W., Pflug, J., Mazzotti, G., Jonas, T., Deems, J., Bormann, K., Painter, T., Hiemstra, C., Gelvin, A., Uhlmann, Z., Spaete, L., Glenn, N., and Lundquist, J.: Comparing Aerial Lidar Observations With Terrestrial Lidar and Snow-Probe Transects From NASA's 2017 SnowEx Campaign, Water Resources Research, 55, 6285-6294, 10.1029/2018WR024533, 2019.~~

~~DeLong, S., Youberg, A., DeLong, W., and Murphy, B.: Post-wildfire landscape change and erosional processes from repeat terrestrial lidar in a steep headwater catchment, Chiricahua Mountains, Arizona, USA, Geomorphology, 300, 13-30, 10.1016/j.geomorph.2017.09.028, 2018.~~

~~Dingman, S. L.: Physical Hydrology, 3, Waveland Press, Inc., Long Grove, IL2015.~~

~~Elder, K., Dozier, J., and Michaelsen, J.: Snow Accumulation and Distribution in an Alpine Watershed, Water Resources Research, 27, 1541-1552, 1991.~~

~~Erickson, T. A., Williams, M. W., and Winstral, A.: Persistence of topographic controls on the spatial distribution of snow in rugged mountain terrain, Colorado, United States, Water Resources Research, 41, Artn W04014 10.1029/2003wr002973, 2005.~~

~~Fassnacht, S. R.: A Call for More Snow Sampling, Geosciences, 11, ARTN 435 10.3390/geosciences11110435, 2021.~~

~~Fassnacht, S. R., Brown, K. S. J., Blumberg, E. J., Moreno, J. I. L., Covino, T. P., Kappas, M., Huang, Y., Leone, V., and Kashipazha, A. H.: Distribution of snow depth variability, Frontiers of Earth Science, 12, 683-692, 10.1007/s11707-018-0714-z, 2018.~~

~~Guiot, A., Karbou, F., James, G., and Durand, P.: Insights into Segmentation Methods Applied to Remote Sensing SAR Images for Wet Snow Detection, Geosciences, 13, ARTN 193 10.3390/geosciences13070193, 2023.~~

~~Hinckley, E.-L. S., Ebel, B. A., Barnes, R. T., Anderson, R. S., Williams, M. W., and Anderson, S. P.: Aspect control of water movement on hillslopes near the rain-snow transition of the Colorado Front Range, Hydrological Processes, 28, 74-85, 10.1002/hyp.9549, 2014.~~

~~Jencso, K. G. and McGlynn, B. L.: Hierarchical controls on runoff generation: Topographically driven hydrologic connectivity, geology, and vegetation, Water Resources Research, 47, W11527, 10.1029/2011wr010666, 2011.~~

~~Jennings, K., Kittel, T., and Molotch, N.: Observations and simulations of the seasonal evolution of snowpack cold content and its relation to snowmelt and the snowpack energy budget, Cryosphere, 12, 1595-1614, 10.5194/tc-12-1595-2018, 2018a.~~

~~Jennings, K., Winchell, T., Livneh, B., and Molotch, N.: Spatial variation of the rain-snow temperature threshold across the Northern Hemisphere, Nature Communications, 9, 10.1038/s41467-018-03629-7, 2018b.~~

~~Kovacs, A., Gow, A. J., and Morey, R. M.: The in-situ dielectric constant of polar firn revisited, Cold Regions Science and Technology, 23, 245-256, https://doi.org/10.1016/0165-232X(94)00016-Q, 1995.~~

~~Li, D., Wrzesien, M., Durand, M., Adam, J., and Lettenmaier, D.: How much runoff originates as snow in the western United States, and how will that change in the future?, Geophysical Research Letters, 44, 6163-6172, 10.1002/2017GL073551, 2017.~~

~~Lopez-Moreno, J., Fassnacht, S., Heath, J., Musselman, K., Revuelto, J., Latron, J., Moran-Tejeda, E., and Jonas, T.: Small scale spatial variability of snow density and depth over complex alpine terrain: Implications for estimating snow water equivalent, Advances in Water Resources, 55, 40-52, 10.1016/j.advwatres.2012.08.010, 2013.~~

~~Lundquist, J., Dickerson-Lange, S., Lutz, J., and Cristea, N.: Lower forest density enhances snow retention in regions with warmer winters: A global framework developed from plot-scale observations and modeling, Water Resources Research, 49, 6356-6370, 10.1002/wrcr.20504, 2013.~~

~~Lundy, C., Brown, R., Adams, E., Birkeland, K., and Lehning, M.: A statistical validation of the snowpack model in a Montana climate, Cold Regions Science and Technology, 33, 237-246, 10.1016/S0165-232X(01)00038-6, 2001.~~

~~Mankin, J., Viviroli, D., Singh, D., Hoekstra, A., and Diffenbaugh, N.: The potential for snow to supply human water demand in the present and future, Environmental Research Letters, 10, 10.1088/1748-9326/10/11/114016, 2015.~~

~~Marks, D., Winstral, A., and Seyfried, M.: Simulation of terrain and forest shelter effects on patterns of snow deposition, snowmelt and runoff over a semi-arid mountain catchment, Hydrological Processes, 16, 3605-3626, 10.1002/hyp.1237, 2002.~~

~~Marshall, H. and Koh, G.: FMCW radars for snow research, Cold Regions Science and Technology, 52, 118-131, 10.1016/j.coldregions.2007.04.008, 2008.~~

~~Marshall, H., Koh, G., Forster, R., and MacAyeal, D.: Estimating alpine snowpack properties using FMCW radar, Annals of Glaciology, Vol 40, 2005, 40, 157-162, 10.3189/172756405781813500, 2005.~~

~~Mcgrath, D., Bonnell, R., Zeller, L., Olsen-Mikitowicz, A., Bump, E., Webb, R., and Marshall, H. P.: A Time Series of Snow Density and Snow Water Equivalent Observations Derived From the Integration of GPR and UAV SfM Observations, Frontiers in Remote Sensing, 3, ARTN 886747 10.3389/frsen.2022.886747, 2022.~~

~~McGrath, D., Webb, R., Shean, D., Bonnell, R., Marshall, H., Painter, T., Molotch, N., Elder, K., Hiemstra, C., and Brucker, L.: Spatially extensive ground-penetrating radar snow depth observations during NASA's 2017 SnowEx Campaign: Comparison with in situ, airborne, and satellite observations, Water Resources Research, 10.1029/2019WR024907, 2019.~~

~~McNamara, J. P., Chandler, D., Seyfried, M., and Achet, S.: Soil moisture states, lateral flow, and streamflow generation in a semi-arid, snowmelt-driven catchment, Hydrological Processes, 19, 4023-4038, 10.1002/hyp.5869, 2005.~~

~~Meromy, L., Molotch, N. P., Williams, M. W., Musselman, K. N., and Kueppers, L. M.: Snowpack-climate manipulation using infrared heaters in subalpine forests of the Southern Rocky Mountains, USA, Agricultural and Forest Meteorology, 203, 142-157, https://doi.org/10.1016/j.agrformet.2014.12.015, 2015.~~

~~Modi, P. A., Small, E. E., Kasprzyk, J., and Livneh, B.: Investigating the Role of Snow Water Equivalent on Streamflow Predictability during Drought, Journal of Hydrometeorology, 23, 1607-1625, 10.1175/Jhm-D-21-0229.1, 2022.~~

~~Molotch, N. P. and Meromy, L.: Physiographic and climatic controls on snow cover persistence in the Sierra Nevada Mountains, Hydrological Processes, 28, 4573-4586, 10.1002/hyp.10254, 2014.~~

~~Musselman, K. N., Molotch, N. P., and Brooks, P. D.: Effects of vegetation on snow accumulation and ablation in a mid-latitude sub-alpine forest, Hydrological Processes, 22, 2767-2776, 10.1002/hyp.7050, 2008.~~

~~Musselman, K. N., Molotch, N. P., Margulis, S. A., Kirchner, P. B., and Bales, R. C.: Influence of canopy structure and direct beam solar irradiance on snowmelt rates in a mixed conifer forest, Agricultural and Forest Meteorology, 161, 46-56, 10.1016/j.agrformet.2012.03.011, 2012.~~

~~Nolin, A. W., Sproles, E. A., Rupp, D. E., Crumley, R. L., Webb, M. J., Palomaki, R. T., and Mar, E.: New snow metrics for a warming world, Hydrological Processes, 35, ARTN e14262~~
~~10.1002/hyp.14262, 2021.~~

~~Painter, T., Berisford, D., Boardman, J., Bormann, K., Deems, J., Gehrke, F., Hedrick, A., Joyce, M., Laidlaw, R., Marks, D., Mattmann, C., McGurk, B., Ramirez, P., Richardson, M., Skiles, S., Seidel, F., and Winstral, A.: The Airborne Snow Observatory: Fusion of scanning lidar, imaging spectrometer, and physically-based modeling for mapping snow water equivalent and snow albedo, Remote Sensing of Environment, 184, 139-152, 10.1016/j.rse.2016.06.018, 2016.~~

~~Raleigh, M. and Small, E.: Snowpack density modeling is the primary source of uncertainty when mapping basin-wide SWE with lidar, Geophysical Research Letters, 44, 3700-3709, 10.1002/2016GL071999, 2017.~~

~~Rutter, N., Essery, R., Pomeroy, J., Altimir, N., Andreadis, K., Baker, I., Barr, A., Bartlett, P., Boone, A., Deng, H., Douville, H., Dutra, E., Elder, K., Ellis, C., Feng, X., Gelfan, A., Goodbody, A., Gusev, Y., Gustafsson, D., Hellstrom, R., Hirabayashi, Y., Hirota, T., Jonas, T., Koren, V., Kuragina, A., Lettenmaier, D., Li, W., Luce, C., Martin, E., Nasonova, O., Pumpanen, J., Pyles, R., Samuelsson, P., Sandells, M., Schadler, G., Shmakin, A., Smirnova, T., Stahli, M., Stockli, R., Strasser, U., Su, H., Suzuki, K., Takata, K., Tanaka, K., Thompson, E., Vesala, T., Viterbo, P., Wiltshire, A., Xia, K., Xue, Y., and Yamazaki, T.: Evaluation of forest snow processes models (SnowMIP2), Journal of Geophysical Research-Atmospheres, 114, 10.1029/2008JD011063, 2009.~~

~~Sexstone, G. A. and Fassnacht, S. R.: What drives basin scale spatial variability of snowpack properties in northern Colorado?, The Cryosphere, 8, 329-344, 10.5194/tc-8-329-2014, 2014.~~

~~Skiles, S., Flanner, M., Cook, J., Dumont, M., and Painter, T.: Radiative forcing by light-absorbing particles in snow, Nature Climate Change, 8, 965-+, 10.1038/s41558-018-0296-5, 2018.~~

~~Sommerfeld, R. A. and Rocchio, J. E.: Permeability measurements on new and equitemperature snow, Water Resources Research, 29, 2485-2490, https://doi.org/10.1029/93WR01071, 1993.~~

~~Sturm, M., Goldstein, M., and Parr, C.: Water and life from snow: A trillion dollar science question, Water Resources Research, 53, 3534-3544, 10.1002/2017WR020840, 2017.~~

~~Tarricone, J., Webb, R. W., Marshall, H. P., Nolin, A. W., and Meyer, F. J.: Estimating snow accumulation and ablation with L-band interferometric synthetic aperture radar (InSAR), Cryosphere, 17, 1997-2019, 10.5194/tc-17-1997-2023, 2023.~~

~~Teng, W., Rui, H. L., Strub, R., and Vollmer, B.: Optimal Reorganization of Nasa Earth Science Data for Enhanced Accessibility and Usability for the Hydrology Community, Journal of the American Water Resources Association, 52, 825-835, 10.1111/1752-1688.12405, 2016.~~

~~Valt, M., Guyennon, N., Salerno, F., Petrangeli, A. B., Salvatori, R., Cianfarra, P., and Romano, E.: Predicting new snow density in the Italian Alps: A variability analysis based on 10years of measurements, Hydrological Processes, 32, 3174-3187, 10.1002/hyp.13249, 2018.~~

~~Varhola, A., Coops, N. C., Weiler, M., and Moore, R. D.: Forest canopy effects on snow accumulation and ablation: An integrative review of empirical results, Journal of Hydrology, 392, 219-233, 10.1016/j.jhydrol.2010.08.009, 2010.~~

~~Vionnet, V., Guyomarc'h, G., Naaim Bouvet, F., Martin, E., Durand, Y., Bellot, H., Bel, C., and Puglièse, P.: Occurrence of blowing snow events at an alpine site over a 10-year period: Observations and modelling, Advances in Water Resources, 55, 53-63, https://doi.org/10.1016/j.advwatres.2012.05.004, 2013.~~

~~Webb, R., Jennings, K., Finsterle, S., and Fassnacht, S.: Two-dimensional liquid water flow through snow at the plot scale in continental snowpacks: simulations and field data comparisons, Cryosphere, 15, 1423-1434, 10.5194/tc-15-1423-2021, 2021a.~~

~~Webb, R. W.: Using ground penetrating radar to assess the variability of snow water equivalent and melt in a mixed canopy forest, Northern Colorado, Frontiers of Earth Science, 11, 482-495, 10.1007/s11707-017-0645-0, 2017.~~

~~Webb, R. W., Fassnacht, S. R., and Gooseff, M. N.: Hydrologic flow path development varies by aspect during spring snowmelt in complex subalpine terrain, Cryosphere, 12, 287-300, 10.5194/tc-12-287-2018, 2018a.~~

~~Webb, R. W., Litvak, M. E., and Brooks, P. D.: The role of terrain-mediated hydroclimate in vegetation recovery after wildfire, Environmental Research Letters, 18, 064036, 10.1088/1748-9326/acd803, 2023.~~

~~Webb, R. W., Fassnacht, S. R., Gooseff, M. N., and Webb, S. W.: The Presence of Hydraulic Barriers in Layered Snowpacks: TOUGH2 Simulations and Estimated Diversion Lengths, Transport in Porous Media, 123, 457-476, 10.1007/s11242-018-1079-1, 2018b.~~

~~Webb, R. W., Jennings, K., Fend, M., and Molotch, N.: Combining Ground Penetrating Radar with Terrestrial LiDAR Scanning to Estimate the Spatial Distribution of Liquid Water Content in Seasonal Snowpacks, Water Resources Research, 54, 10339-10349, 10.1029/2018WR022680, 2018c.~~

~~Webb, R. W., Musselman, K. N., Ciafone, S., Hale, K. E., and Molotch, N. P.: Extending the vadose zone: Characterizing the role of snow for liquid water storage and transmission in streamflow generation, Hydrological Processes, 36, e14541, https://doi.org/10.1002/hyp.14541, 2022.~~

~~Webb, R. W., Wigmore, O., Jennings, K., Fend, M., and Molotch, N. P.: Hydrologic connectivity at the hillslope scale through intra-snowpack flow paths during snowmelt, Hydrological Processes, 34, 1616-1629, 10.1002/hyp.13686, 2020a.~~

~~Webb, R. W., Marziliano, A., McGrath, D., Bonnell, R., Meehan, T. G., Vuyovich, C., and Marshall, H.-P.: In Situ Determination of Dry and Wet Snow Permittivity: Improving Equations for Low Frequency Radar Applications, Remote Sensing, 13, 4617, 2021b.~~

~~Webb, R. W., Raleigh, M. S., McGrath, D., Molotch, N. P., Elder, K., Hiemstra, C., Brucker, L., and Marshall, H. P.: Within-Stand Boundary Effects on Snow Water Equivalent Distribution in Forested Areas, Water Resources Research, 56, e2019WR024905, 10.1029/2019wr024905, 2020b.~~

~~Wever, N., Fierz, C., Mitterer, C., Hirashima, H., and Lehning, M.: Solving Richards Equation for snow improves snowpack meltwater runoff estimations in detailed multi-layer snowpack model, Cryosphere, 8, 257-274, 10.5194/tc-8-257-2014, 2014.~~

~~Winstral, A., Elder, K., and Davis, R. E.: Spatial snow modeling of wind-redistributed snow using terrain-based parameters, Journal of Hydrometeorology, 3, 524-538, Doi 10.1175/1525-7541(2002)003<0524:Ssmowr>2.0.Co;2, 2002.~~

~~Xia, Y. L., Mitchell, K., Ek, M., Sheffield, J., Cosgrove, B., Wood, E., Luo, L. F., Alonge, C., Wei, H. L., Meng, J., Livneh, B., Lettenmaier, D., Koren, V., Duan, Q. Y., Mo, K., Fan, Y., and Mocko, D.: Continental-scale water and energy flux analysis and validation for the North American Land Data Assimilation System project phase 2 (NLDAS-2): 1. Intercomparison and application of model products, Journal of Geophysical Research-Atmospheres, 117, Artn D03109 10.1029/2011jd016048, 2012.~~

~~Zeinivand, H. and De Smedt, F.: Prediction of snowmelt floods with a distributed hydrological model using a physical snow mass and energy balance approach, Natural Hazards, 54, 451-468, 10.1007/s11069-009-9478-9, 2010.~~

Bales, R. C., Molotch, N. P., Painter, T. H., Dettinger, M. D., Rice, R., and Dozier, J.: Mountain hydrology of the western United States, Water Resources Research, 42, W08432, 10.1029/2005wr004387, 2006.

Bartelt, P. and Lehning, M.: A physical SNOWPACK model for the Swiss avalanche warning Part I: numerical model, Cold Regions Science and Technology, 35, 123-145, 10.1016/S0165-232X(02)00074-5, 2002.

Bishay, K., Bjarke, N. R., Modi, P., Pflug, J. M., and Livneh, B.: Can Remotely Sensed Snow Disappearance Explain Seasonal Water Supply?, Water, 15, ARTN 1147, 10.3390/w15061147, 2023.

Bonnell, R., McGrath, D., Williams, K., Webb, R., Fassnacht, S. R., and Marshall, H.-P.: Spatiotemporal Variations in Liquid Water Content in a Seasonal Snowpack: Implications for Radar Remote Sensing, Remote Sensing, 13, 4223, 2021.

Bradford, J., Harper, J., and Brown, J.: Complex dielectric permittivity measurements from ground-penetrating radar data to estimate snow liquid water content in the pendular regime, Water Resources Research, 45, 10.1029/2008WR007341, 2009.

Brooks, P. D., Gelderloos, A., Wolf, M. A., Jamison, L. R., Strong, C., Solomon, D. K., Bowen, G. J., Burian, S., Tai, X., Arens, S., Briefer, L., Kirkham, T., and Stewart, J.: Groundwater-Mediated Memory of Past Climate Controls Water Yield in Snowmelt-Dominated Catchments, Water Resources Research, 57, e2021WR030605, https://doi.org/10.1029/2021WR030605, 2021.

Clow, D. W.: Changes in the Timing of Snowmelt and Streamflow in Colorado: A Response to Recent Warming, Journal of Climate, 23, 2293-2306, 10.1175/2009jcli2951.1, 2010.

Co, M.: Colorado Hazard Mapping: LiDAR [dataset], 2016.

Currier, W., Pflug, J., Mazzotti, G., Jonas, T., Deems, J., Bormann, K., Painter, T., Hiemstra, C., Gelvin, A., Uhlmann, Z., Spaete, L., Glenn, N., and Lundquist, J.: Comparing Aerial Lidar Observations With Terrestrial Lidar and Snow-Probe Transects From NASA's 2017 SnowEx Campaign, Water Resources Research, 55, 6285-6294, 10.1029/2018WR024533, 2019.

Díaz, C. L. P., Muñoz, J., Lakhankar, T., Khanbilvardi, R., and Romanov, P.: Proof of Concept: Development of Snow Liquid Water Content Profiler Using CS650 Reflectometers at Caribou, ME, USA, Sensors, 17, ARTN 647 10.3390/s17030647, 2017.

Dingman, S. L.: Physical Hydrology, 3, Waveland Press, Inc., Long Grove, IL2015.

Elder, K., Dozier, J., and Michaelsen, J.: Snow Accumulation and Distribution in an Alpine Watershed, Water Resources Research, 27, 1541-1552, 1991.

Eiriksson, D., Whitson, M., Luce, C. H., Marshall, H. P., Bradford, J., Benner, S. G., Black, T., Hetrick, H., and McNamara, J. P.: An evaluation of the hydrologic relevance of lateral flow in snow at hillslope and catchment scales, Hydrological Processes, 27, 640-654, 10.1002/hyp.9666, 2013.

Erickson, T. A., Williams, M. W., and Winstral, A.: Persistence of topographic controls on the spatial distribution of snow in rugged mountain terrain, Colorado, United States, Water Resources Research, 41, Artn W04014 10.1029/2003wr002973, 2005.

Fassnacht, S. R.: A Call for More Snow Sampling, Geosciences, 11, ARTN 435, 10.3390/geosciences11110435, 2021.

Fassnacht, S. R., Brown, K. S. J., Blumberg, E. J., Moreno, J. I. L., Covino, T. P., Kappas, M., Huang, Y., Leone, V., and Kashipazha, A. H.: Distribution of snow depth variability, Frontiers of Earth Science, 12, 683-692, 10.1007/s11707-018-0714-z, 2018.

Guiot, A., Karbou, F., James, G., and Durand, P.: Insights into Segmentation Methods Applied to Remote Sensing SAR Images for Wet Snow Detection, Geosciences, 13, ARTN 193 10.3390/geosciences13070193, 2023.

Heilig, A., Mitterer, C., Schmid, L., Wever, N., Schweizer, J., Marshall, H. P., and Eisen, O.: Seasonal and diurnal cycles of liquid water in snow-Measurements and modeling, Journal of Geophysical Research: Earth Surface, 120, 2139-2154, 10.1002/2015JF003593, 2015.

Hinckley, E.-L. S., Ebel, B. A., Barnes, R. T., Anderson, R. S., Williams, M. W., and Anderson, S. P.: Aspect control of water movement on hillslopes near the rain-snow transition of the Colorado Front Range, Hydrological Processes, 28, 74-85, 10.1002/hyp.9549, 2014.

Jencso, K. G. and McGlynn, B. L.: Hierarchical controls on runoff generation: Topographically driven hydrologic connectivity, geology, and vegetation, Water Resources Research, 47, W11527, 10.1029/2011wr010666, 2011.

Jennings, K., Kittel, T., and Molotch, N.: Observations and simulations of the seasonal evolution of snowpack cold content and its relation to snowmelt and the snowpack energy budget, Cryosphere, 12, 1595-1614, 10.5194/tc-12-1595-2018, 2018a.

Jennings, K., Winchell, T., Livneh, B., and Molotch, N.: Spatial variation of the rain-snow temperature threshold across the Northern Hemisphere, Nature Communications, 9, 10.1038/s41467-018-03629-7, 2018b.

Kinar, N. J. and Pomeroy, J. W.: Measurement of the physical properties of the snowpack, Reviews of Geophysics, 53, 481-544, 10.1002/2015rg000481, 2015.

Koch, F., Prasch, M., Schmid, L., Schweizer, J., and Mauser, W.: Measuring Snow Liquid Water Content with Low-Cost GPS Receivers, Sensors, 14, 20975-20999, 10.3390/s141120975, 2014.

Kovacs, A., Gow, A. J., and Morey, R. M.: The in-situ dielectric constant of polar firn revisited, Cold Regions Science and Technology, 23, 245-256, https://doi.org/10.1016/0165-232X(94)00016-Q, 1995.

Li, D., Wrzesien, M., Durand, M., Adam, J., and Lettenmaier, D.: How much runoff originates as snow in the western United States, and how will that change in the future?, Geophysical Research Letters, 44, 6163-6172, 10.1002/2017GL073551, 2017.

López-Moreno, J. I., Fassnacht, S. R., Beguería, S., and Latron, J. B. P.: Variability of snow depth at the plot scale: implications for mean depth estimation and sampling strategies, The Cryosphere, 5, 617-629, 10.5194/tc-5-617-2011, 2011.

López-Moreno, J., Fassnacht, S., Heath, J., Musselman, K., Revuelto, J., Latron, J., Moran-Tejeda, E., and Jonas, T.: Small scale spatial variability of snow density and depth over complex alpine terrain: Implications for estimating snow water equivalent, Advances in Water Resources, 55, 40-52, 10.1016/j.advwatres.2012.08.010, 2013.

Lundquist, J., Dickerson-Lange, S., Lutz, J., and Cristea, N.: Lower forest density enhances snow retention in regions with warmer winters: A global framework developed from plot-scale observations and modeling, Water Resources Research, 49, 6356-6370, 10.1002/wrcr.20504, 2013.

Lundy, C., Brown, R., Adams, E., Birkeland, K., and Lehning, M.: A statistical validation of the snowpack model in a Montana climate, Cold Regions Science and Technology, 33, 237-246, 10.1016/S0165-232X(01)00038-6, 2001.

Marks, D., Winstral, A., and Seyfried, M.: Simulation of terrain and forest shelter effects on patterns of snow deposition, snowmelt and runoff over a semi-arid mountain catchment, Hydrological Processes, 16, 3605-3626, 10.1002/hyp.1237, 2002.

Marshall, H. and Koh, G.: FMCW radars for snow research, Cold Regions Science and Technology, 52, 118-131, 10.1016/j.coldregions.2007.04.008, 2008.

Marshall, H., Koh, G., Forster, R., and MacAyeal, D.: Estimating alpine snowpack properties using FMCW radar, Annals of Glaciology, Vol 40, 2005, 40, 157-162, 10.3189/172756405781813500, 2005.

Mazzotti, G., Webster, C., Quéno, L., Cluzet, B., and Jonas, T.: Canopy structure, topography, and weather are equally important drivers of small-scale snow cover dynamics in sub-alpine forests, Hydrology and Earth System Sciences, 27, 2099-2121, 10.5194/hess-27-2099-2023, 2023.

Mcgrath, D., Bonnell, R., Zeller, L., Olsen-Mikitowicz, A., Bump, E., Webb, R., and Marshall, H. P.: A Time Series of Snow Density and Snow Water Equivalent Observations Derived From the Integration of GPR and UAV SfM Observations, Frontiers in Remote Sensing, 3, ARTN 886747, 10.3389/frsen.2022.886747, 2022.

McGrath, D., Webb, R., Shean, D., Bonnell, R., Marshall, H., Painter, T., Molotch, N., Elder, K., Hiemstra, C., and Brucker, L.: Spatially extensive ground-penetrating radar snow depth observations during NASA's 2017 SnowEx Campaign: Comparison with in situ, airborne, and satellite observations, Water Resources Research, 10.1029/2019WR024907, 2019.

McNamara, J. P., Chandler, D., Seyfried, M., and Achet, S.: Soil moisture states, lateral flow, and streamflow generation in a semi-arid, snowmelt-driven catchment, Hydrological Processes, 19, 4023-4038, 10.1002/hyp.5869, 2005.

Meehan, T. G., Hojatimalekshah, A., Marshall, H.-P., Deeb, E. J., O'Neel, S., McGrath, D., Webb, R. W., Bonnell, R., Raleigh, M. S., Hiemstra, C., and Elder, K.: Spatially distributed snow depth, bulk density, and snow water equivalent from ground-based and airborne sensor integration at Grand Mesa, Colorado, USA, *The Cryosphere*, 18, 3253–3276, https://doi.org/10.5194/tc-18-3253-2024, 2024.

Meromy, L., Molotch, N. P., Williams, M. W., Musselman, K. N., and Kueppers, L. M.: Snowpack-climate manipulation using infrared heaters in subalpine forests of the Southern Rocky Mountains, USA, Agricultural and Forest Meteorology, 203, 142-157, https://doi.org/10.1016/j.agrformet.2014.12.015, 2015.

Mitterer, C., Heilig, A., Sweizer, J., and Eisen, O.: Upward-looking ground-penetrating radar for measuring wet-snow properties, Cold Regions Science and Technology, 69, 129-138, 10.1016/j.coldregions.2011.06.003, 2011.

Modi, P. A., Small, E. E., Kasprzyk, J., and Livneh, B.: Investigating the Role of Snow Water Equivalent on Streamflow Predictability during Drought, Journal of Hydrometeorology, 23, 1607-1625, 10.1175/Jhm-D-21-0229.1, 2022.

Molotch, N. P. and Meromy, L.: Physiographic and climatic controls on snow cover persistence in the Sierra Nevada Mountains, Hydrological Processes, 28, 4573-4586, 10.1002/hyp.10254, 2014.

Musselman, K. N., Molotch, N. P., and Brooks, P. D.: Effects of vegetation on snow accumulation and ablation in a mid-latitude sub-alpine forest, Hydrological Processes, 22, 2767-2776, 10.1002/hyp.7050, 2008.

Musselman, K. N., Molotch, N. P., Margulis, S. A., Kirchner, P. B., and Bales, R. C.: Influence of canopy structure and direct beam solar irradiance on snowmelt rates in a mixed conifer forest, Agricultural and Forest Meteorology, 161, 46-56, 10.1016/j.agrformet.2012.03.011, 2012.

Nolin, A. W., Sproles, E. A., Rupp, D. E., Crumley, R. L., Webb, M. J., Palomaki, R. T., and Mar, E.: New snow metrics for a warming world, Hydrological Processes, 35, ARTN e14262
10.1002/hyp.14262, 2021.

Painter, T., Berisford, D., Boardman, J., Bormann, K., Deems, J., Gehrke, F., Hedrick, A., Joyce, M., Laidlaw, R., Marks, D., Mattmann, C., McGurk, B., Ramirez, P., Richardson, M., Skiles, S., Seidel, F., and Winstral, A.: The Airborne Snow Observatory: Fusion of scanning lidar, imaging spectrometer, and physically-based modeling for mapping snow water equivalent and snow albedo, Remote Sensing of Environment, 184, 139-152, 10.1016/j.rse.2016.06.018, 2016.

Raleigh, M. and Small, E.: Snowpack density modeling is the primary source of uncertainty when mapping basin-wide SWE with lidar, Geophysical Research Letters, 44, 3700-3709, 10.1002/2016GL071999, 2017.

Rutter, N., Essery, R., Pomeroy, J., Altimir, N., Andreadis, K., Baker, I., Barr, A., Bartlett, P., Boone, A., Deng, H., Douville, H., Dutra, E., Elder, K., Ellis, C., Feng, X., Gelfan, A., Goodbody, A., Gusev, Y., Gustafsson, D., Hellstrom, R., Hirabayashi, Y., Hirota, T., Jonas, T., Koren, V., Kuragina, A., Lettenmaier, D., Li, W., Luce, C., Martin, E., Nasonova, O., Pumpanen, J., Pyles, R., Samuelsson, P., Sandells, M., Schadler, G., Shmakin, A., Smirnova, T., Stahli, M., Stockli, R., Strasser, U., Su, H., Suzuki, K., Takata, K., Tanaka, K., Thompson, E., Vesala, T., Viterbo, P., Wiltshire, A., Xia, K., Xue, Y., and Yamazaki, T.: Evaluation of forest snow processes models (SnowMIP2), Journal of Geophysical Research-Atmospheres, 114, 10.1029/2008JD011063, 2009.

Schlumpf, M., Hendrikx, J., Stormont, J., and Webb, R.: Quantifying short-term changes in snow strength due to increasing liquid water content above hydraulic barriers, Cold Regions Science and Technology, 218, ARTN 104056, 10.1016/j.coldregions.2023.104056, 2024.

Schmid, L., Koch, F., Heilig, A., Prasch, M., Eisen, O., Mauser, W., and Schweizer, J.: A novel sensor combination (upGPR-GPS) to continuously and nondestructively derive snow cover properties, Geophysical Research Letters, 42, 3397-3405, 10.1002/2015GL063732, 2015.

Sexstone, G. A. and Fassnacht, S. R.: What drives basin scale spatial variability of snowpack properties in northern Colorado?, The Cryosphere, 8, 329-344, 10.5194/tc-8-329-2014, 2014.

Skiles, S., Flanner, M., Cook, J., Dumont, M., and Painter, T.: Radiative forcing by light-absorbing particles in snow, Nature Climate Change, 8, 965-+, 10.1038/s41558-018-0296-5, 2018.

Sommerfeld, R. A. and Rocchio, J. E.: Permeability measurements on new and equitemperature snow, Water Resources Research, 29, 2485-2490, https://doi.org/10.1029/93WR01071, 1993.

Sturm, M., Goldstein, M., and Parr, C.: Water and life from snow: A trillion dollar science question, Water Resources Research, 53, 3534-3544, 10.1002/2017WR020840, 2017.

Tarricone, J., Webb, R. W., Marshall, H. P., Nolin, A. W., and Meyer, F. J.: Estimating snow accumulation and ablation with L-band interferometric synthetic aperture radar (InSAR), Cryosphere, 17, 1997-2019, 10.5194/tc-17-1997-2023, 2023.

Teng, W., Rui, H. L., Strub, R., and Vollmer, B.: Optimal Reorganization of Nasa Earth Science Data for Enhanced Accessibility and Usability for the Hydrology Community, Journal of the American Water Resources Association, 52, 825-835, 10.1111/1752-1688.12405, 2016.

Thompson, S., Kulessa, B., Essery, R., and Luthi, M.: Bulk meltwater flow and liquid water content of snowpacks mapped using the electrical self-potential (SP) method, Cryosphere, 10, 433-444, 10.5194/tc-10-433-2016, 2016.

Valt, M., Guyennon, N., Salerno, F., Petrangeli, A. B., Salvatori, R., Cianfarra, P., and Romano, E.: Predicting new snow density in the Italian Alps: A variability analysis based on 10years of measurements, Hydrological Processes, 32, 3174-3187, 10.1002/hyp.13249, 2018.

Varhola, A., Coops, N. C., Weiler, M., and Moore, R. D.: Forest canopy effects on snow accumulation and ablation: An integrative review of empirical results, Journal of Hydrology, 392, 219-233, 10.1016/j.jhydrol.2010.08.009, 2010.

Vionnet, V., Guyomarc'h, G., Naaim Bouvet, F., Martin, E., Durand, Y., Bellot, H., Bel, C., and Puglièse, P.: Occurrence of blowing snow events at an alpine site over a 10-year period: Observations and modelling, Advances in Water Resources, 55, 53-63, https://doi.org/10.1016/j.advwatres.2012.05.004, 2013.

Webb, R., Jennings, K., Finsterle, S., and Fassnacht, S.: Two-dimensional liquid water flow through snow at the plot scale in continental snowpacks: simulations and field data comparisons, Cryosphere, 15, 1423-1434, 10.5194/tc-15-1423-2021, 2021a.

Webb, R. W.: Using ground penetrating radar to assess the variability of snow water equivalent and melt in a mixed canopy forest, Northern Colorado, Frontiers of Earth Science, 11, 482-495, 10.1007/s11707-017-0645-0, 2017.

Webb, R. W., Fassnacht, S. R., and Gooseff, M. N.: Hydrologic flow path development varies by aspect during spring snowmelt in complex subalpine terrain, Cryosphere, 12, 287-300, 10.5194/tc-12-287-2018, 2018a.

Webb, R. W., Litvak, M. E., and Brooks, P. D.: The role of terrain-mediated hydroclimate in vegetation recovery after wildfire, Environmental Research Letters, 18, 064036, 10.1088/1748-9326/acd803, 2023.

Webb, R. W., Fassnacht, S. R., Gooseff, M. N., and Webb, S. W.: The Presence of Hydraulic Barriers in Layered Snowpacks: TOUGH2 Simulations and Estimated Diversion Lengths, Transport in Porous Media, 123, 457-476, 10.1007/s11242-018-1079-1, 2018b.

Webb, R. W., Jennings, K., Fend, M., and Molotch, N.: Combining Ground Penetrating Radar with Terrestrial LiDAR Scanning to Estimate the Spatial Distribution of Liquid Water Content in Seasonal Snowpacks, Water Resources Research, 54, 10339-10349, 10.1029/2018WR022680, 2018c.

Webb, R. W., Musselman, K. N., Ciafone, S., Hale, K. E., and Molotch, N. P.: Extending the vadose zone: Characterizing the role of snow for liquid water storage and transmission in streamflow generation, Hydrological Processes, 36, e14541, https://doi.org/10.1002/hyp.14541, 2022.

Webb, R. W., Wigmore, O., Jennings, K., Fend, M., and Molotch, N. P.: Hydrologic connectivity at the hillslope scale through intra-snowpack flow paths during snowmelt, Hydrological Processes, 34, 1616-1629, 10.1002/hyp.13686, 2020a.

Webb, R. W., Marziliano, A., McGrath, D., Bonnell, R., Meehan, T. G., Vuyovich, C., and Marshall, H.-P.: In Situ Determination of Dry and Wet Snow Permittivity: Improving Equations for Low Frequency Radar Applications, Remote Sensing, 13, 4617, 2021b.

Webb, R. W., Raleigh, M. S., McGrath, D., Molotch, N. P., Elder, K., Hiemstra, C., Brucker, L., and Marshall, H. P.: Within-Stand Boundary Effects on Snow Water Equivalent Distribution in Forested Areas, Water Resources Research, 56, e2019WR024905, 10.1029/2019wr024905, 2020b.

Wever, N., Fierz, C., Mitterer, C., Hirashima, H., and Lehning, M.: Solving Richards Equation for snow improves snowpack meltwater runoff estimations in detailed multi-layer snowpack model, Cryosphere, 8, 257-274, 10.5194/tc-8-257-2014, 2014.

Winstral, A., Elder, K., and Davis, R. E.: Spatial snow modeling of wind-redistributed snow using terrain-based parameters, Journal of Hydrometeorology, 3, 524-538, Doi 10.1175/1525-7541(2002)003<0524:Ssmowr>2.0.Co;2, 2002.

Würzer, S., Wever, N., Juras, R., Lehning, M., and Jonas, T.: Modelling liquid water transport in snow under rain-on-snow conditions - considering preferential flow, Hydrology and Earth System Sciences, 21, 1741-1756, 10.5194/hess-21-1741-2017, 2017.

Xia, Y. L., Mitchell, K., Ek, M., Sheffield, J., Cosgrove, B., Wood, E., Luo, L. F., Alonge, C., Wei, H. L., Meng, J., Livneh, B., Lettenmaier, D., Koren, V., Duan, Q. Y., Mo, K., Fan, Y., and Mocko, D.: Continental-scale water and energy flux analysis and validation for the North American Land Data Assimilation System project phase 2 (NLDAS-2): 1. Intercomparison and application of model products, Journal of Geophysical Research-Atmospheres, 117, Artn D03109, 10.1029/2011jd016048, 2012.

Zeinivand, H. and De Smedt, F.: Prediction of snowmelt floods with a distributed hydrological model using a physical snow mass and energy balance approach, Natural Hazards, 54, 451-468, 10.1007/s11069-009-9478-9, 2010.

Formatted: EndNote Bibliography, Indent: Left: 0", Hanging: 0.5", Line spacing: 1.5 lines